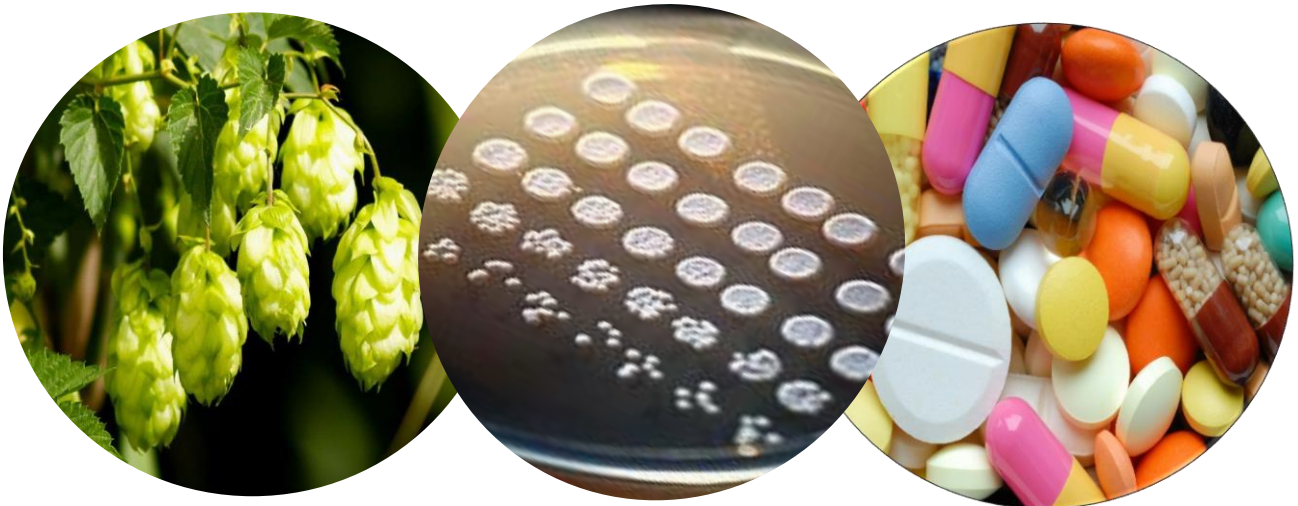


Engineering of *Saccharomyces cerevisiae* towards production of prenylated flavonoids



Menno van der Heide

MSc Biotechnology

Registration number: 931207317040

Examiner a: Dr. Mark Levisson

Examiner b: Dr. Jules Beekwilder

Laboratory of Plant Physiology

Wageningen University

Abstract

Prenylated flavonoids are rare natural products that display a key role in the plants defense mechanism against pathogenic microorganisms. These bioactive compounds exhibit diverse pharmacological activities, such as antimicrobial activity, antioxidant activity, estrogenic activity and antitumor activity. The pharmacological activities are attributed to the presence of prenyl side chains on the various flavonoids. However, due to the fact that prenylated flavonoids are formed rarely in nature, pharmaceutical and nutraceutical applications are still limited. Biosynthesis of prenylated flavonoids using *Saccharomyces cerevisiae* expressing flavonoid biosynthesis genes offers a promising production platform for natural prenylated flavonoids. Via metabolic engineering of this flavonoid biosynthetic pathway, introducing efficient flavonoid prenyltransferases, flavonoids can be prenylated. Therefore, the aim of this work was to create a yeast expression platform for *de novo* production of prenylated flavonoids. We achieved production of the prenylated flavonoids xanthohumol and 8-prenylnaringenin in metabolically engineered *S. cerevisiae*. However, as xanthohumol was only produced through supplementation of the substrate naringenin chalcone, no *de novo* production of xanthohumol could be observed. This study is the first to demonstrate *de novo* production of 8-prenylnaringenin using *S. cerevisiae* expressing a flavonoid prenyltransferase from *Sophora flavescens*, *SfFPT*.

Introduction

Flavonoids are plant secondary metabolites, that can be found ubiquitously in the plant kingdom. These polyphenolic compounds, over which 9000 have been reported so far, are synthesized in plants for a wide variety of purposes: flower colour and aroma, attracting pollinators, acting as a UV-filter and for protection against other abiotic and biotic stresses, leading to strong antimicrobial and antifungal effects (1-4). Additionally, due the presence of hydroxyl groups, flavonoids show even more attractively characteristics such as antioxidant, anti-inflammatory and anti-carcinogenic activity (5, 6). Therefore, an increasing amount of attention is currently being payed to these compounds to study their exact working mechanism and the related health benefits. Flavonoid consumption has been associated with an cardio protective effect, lowering the risk of cardiovascular diseases due to antioxidant and radical scavenging activities (7, 8). Flavonoids also affect the immune system by inducing enzyme systems that are involved in inflammatory responses (9). More specifically, the protein kinases and especially tyrosine and serine-threonine protein kinases, involved in signal transduction and cell activation processes, are being inhibited upon contact with several flavonoids (10, 11). These health-beneficial effects of flavonoids are therefore especially interesting for pharmaceutical and nutraceutical applications (12).

Flavonoid structure

The large family of flavonoid compounds share a common basic carbon skeleton, which consists of two phenyl rings (A- and B-ring) and a heterocyclic ring (C-ring) (Fig. 1). The diverse structures of the flavonoids and their related (pharmacological) properties can be attributed to differences in the heterocyclic ring saturation, hydroxylation patterns and the B ring position (13). Based on these differences, flavonoids can be classified into several subgroups, such as chalcones, flavones and anthocyanins. Additionally, flavonoids can be further modified via methoxylation, C- and O-glycosylation and prenylation.

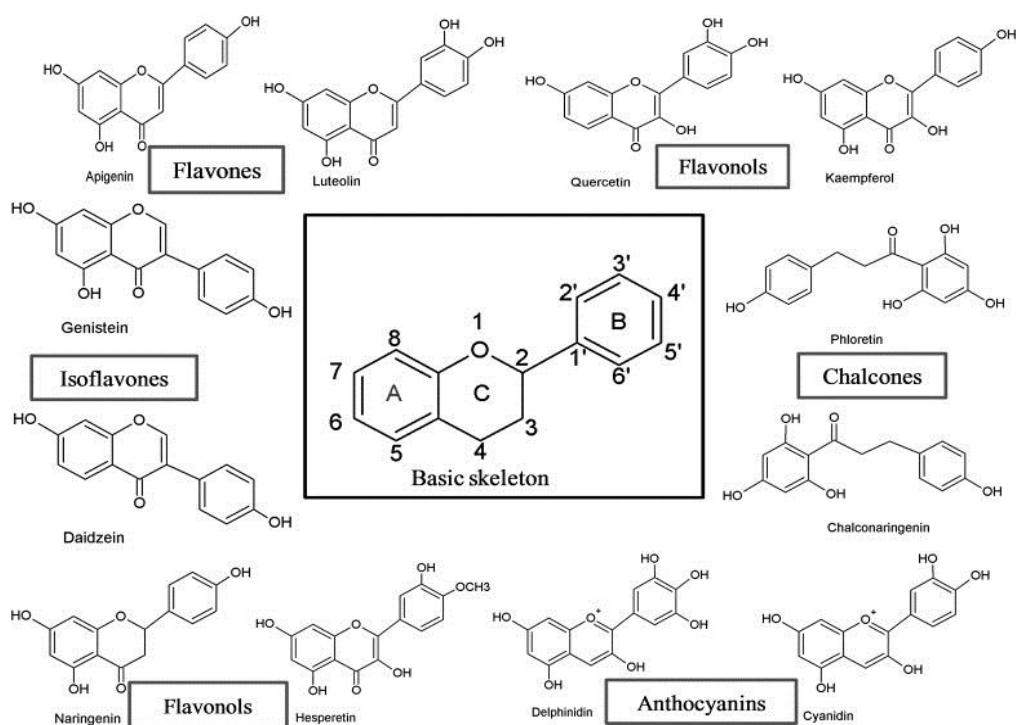


Figure 1. Basic flavonoid structure and flavonoid subgroups.

Prenylated Flavonoids

Prenylated flavonoids are one of the subclasses of flavonoids, although they are far less found in the plant kingdom. This subclass consists of the basic flavonoid carbon skeleton and an isoprenoid side chain, mostly attached to ring A or B. *O*-prenylated flavonoids can also be synthesized, however the occurrence of these compounds in nature is quite limited (14). *C*-prenylation on ring A usually occurs at C-6' and C-8', while *C*-prenylation on ring B occurs at C-3' and C-5'.

Plants containing these prenylated forms of flavonoids are mainly medicinal plants from the Fabaceae, Moraceae and Cannabaceae families (15-17). Prenylation of flavonoids is catalyzed by plant prenyltransferases and can function as a natural defense system against pathogenic bacteria and fungi (18). Besides plant prenyltransferases, also a number of microbial prenyltransferases have been characterized and shown to produce prenylated compounds *in vitro* (19-21). Prenylated compounds may be synthesized in plants upon oxidative stress considering their strong anti-oxidant activity (22). Not only does the prenylated flavonoid improve the plants survivability under abiotic and biotic stress conditions, but the prenyl side chain also improves the biological activities of the flavonoid (23).

Antibacterial activity against Gram positive and negative bacteria was found to be such an improved biological activity. Prenylated phenolic compounds showed low minimum inhibitory concentrations ($\leq 15 \mu\text{g/ml}$), a general >10-fold decrease in value when compared to non-prenylated flavonoids (24). Araya-Cloutier et al. (2017) also found that the position of prenyl groups and the presence of hydroxyl groups affects the antimicrobial activity of

prenylated flavonoids. These prenylated compounds have a broad spectrum of activity and are proposed to have a different mode of action compared to currently used antibacterials. These attributes make prenylated flavonoids promising new antibacterial agents to be used as treatment for bacterial infections, but also as a natural food preservative. The improved bioactivities among the prenylated forms of flavonoids are thought to originate from an increase in lipophilic chain length, enhancing the flavonoids skeleton function. This enhancement leads to a stronger affinity to biological membranes and a more efficient interaction with target proteins, which makes prenylated flavonoids interesting novel nutraceutical and drug candidates (18, 25).

Prenylated flavonoids with interesting biological activities have been identified in hops (*Humulus Lupulus*), of which 8-prenylnaringenin and xanthohumol (Fig. 2) show favourable pharmacological properties (26, 27). Xanthohumol is the major prenylated flavonoid found in the hop cones and shows a broad range of pharmacological properties. 8-Prenylnaringenin is detected in far smaller amounts, but has been described as the most potent phytoestrogen thus far. Xanthohumol shows antibacterial, antioxidant and anti-inflammatory activities, much like most of the flavonoids (28, 29). It's ability to inhibit nuclear factor (NF)- κ B activity, through which T cell proliferation is inhibited, contributes to the anti-inflammatory effects of xanthohumol (29). Furthermore, it was shown that xanthohumol can inhibit tumor cell proliferation and induce apoptosis in various cancer cells via the downregulation of NF- κ B activation (30, 31). These properties make xanthohumol especially attractive as a chemopreventive agent and also as a potential drug for cancer treatment. 8-Prenylnaringenin is able to exert a strong estrogenic activity at low concentrations, when competing with 17 β -estradiol for the binding of estrogen receptors α and β (32). However, at higher concentrations, treatment of breast cancer cells with 8-prenylnaringenin shows cell growth inhibition and even apoptosis in these cells (33). This biphasic effect on cell proliferation can be observed among many phytoestrogens and indicates the importance of pharmacological dosage studies (34). Taken together, the estrogenic properties of 8-prenylnaringenin give a promising view for hormone replacement therapies.

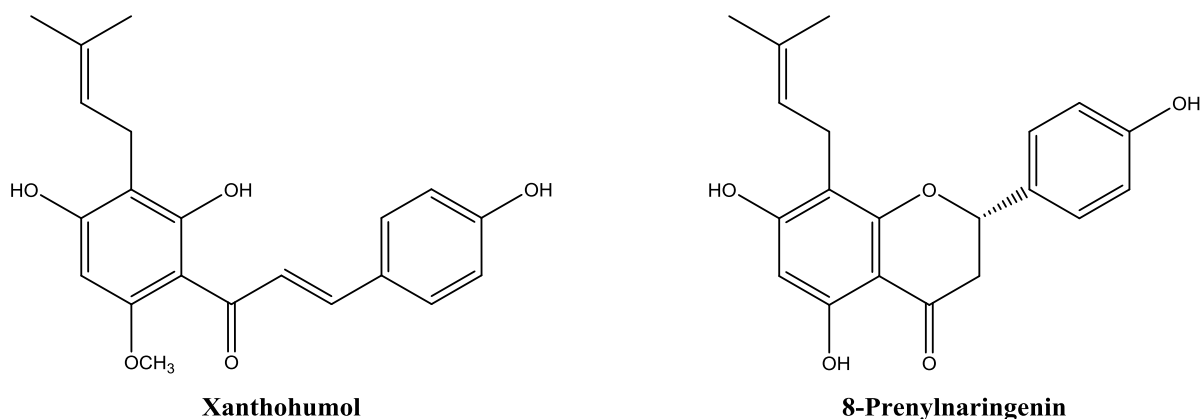


Figure 2. Chemical structures of hop flavonoids xanthohumol and 8-prenylnaringenin.

Flavonoid Biosynthesis

Beer consumption is the main source of dietary intake of both xanthohumol and 8-prenylnaringenin, although only small fractions of the flavonoids remain in the beer after the brewing process. These amounts are insufficient to have significant health-beneficial effects on humans and therefore sufficient production of these prenylated flavonoids is needed to improve the nutritional impact and to particularly test their potential as therapeutic drugs. Although prenylated flavonoids can be isolated from plants, plant-based production of prenylated flavonoids has a low production efficiency and is therefore not suitable for large-scale production (35). Chemical synthesis of prenylated flavonoids is likewise not suitable for large-scale application, considering the low efficiency, complex reactions conditions and the time-consuming process (25).

Biosynthesis of prenylated flavonoids, via metabolic engineering of the flavonoid biosynthetic pathway shows great potential as a production platform. The phenylpropanoid pathway, leading to formation of flavonoids in plants, has already been successfully introduced into the yeast *Saccharomyces cerevisiae* and the bacterium *Escherichia coli* (35-37). These studies showed biotransformation of medium-supplied flavonoid precursors to the flavonoid naringenin, using the enzymes involved in the phenylpropanoid pathway and heterologous expression of naringenin biosynthesis genes. However, *de novo* production of flavonoids is preferred as supplementation with flavonoid precursors becomes impractical for large-scale production, due to high costs (38). Koopman et al. was able to achieve *de novo* production of naringenin, reaching concentrations up to 400 μM in metabolically engineered *S. cerevisiae* (39). These concentrations are a 4-fold increase compared to previous *de novo* biosynthesis of naringenin by engineered *E. coli* (29). A *S. cerevisiae* expression system shows more potential for flavonoid production compared to an *E. coli* expression system. Yeast, as an eukaryotic organism, can posttranslationally modify proteins in a similar way found in plants, thus promoting functional expression of flavonoid-biosynthesis genes (40). Furthermore, a *S. cerevisiae* expression system is efficient, cost effective and offers the possibility to study and control the metabolic flux, which could improve production levels (41). On top of that, biopharmaceutical and nutraceutical production using *S. cerevisiae* is well accepted, because of its GRAS (generally recognized as safe) classification.

Studies on expression of a *Sophora flavescens* prenyltransferase, naringenin 8-dimethylallyltransferase (*SfN8DT-1/SfFPT*), in *S. cerevisiae* showed prenylation of supplemented naringenin, successfully producing 8-prenylnaringenin (42, 43). As for xanthohumol, expression of *Humulus lupulus prenyltransferase 1 (HIPT1)* in insect cells resulted in prenylation of supplemented naringenin chalcone, forming desmethylxanthohumol (44). This compound is converted to xanthohumol by a desmethylxanthohumol 6'-O-methyltransferase (*OMT1*) from *H. lupulus* (45). Similarly, several other flavonoid prenyltransferases, like from *Lupinus albus (LaPT1)* and

Glycine max (*GmG4DT*), have been successfully expressed in *S. cerevisiae* by showing prenyltransferase activity (46, 47).

These previous studies demonstrate the possibility to produce prenylated flavonoids in a yeast expression system, capable of processing eukaryotic proteins. Yet, to date, no *de novo* production of xanthohumol and 8-prenylnaringenin has been achieved in *S. cerevisiae*.

Therefore, in this study we aimed to create a yeast expression platform for *de novo* production of prenylated flavonoids via metabolic engineering of the flavonoid production pathway (Fig. 3).

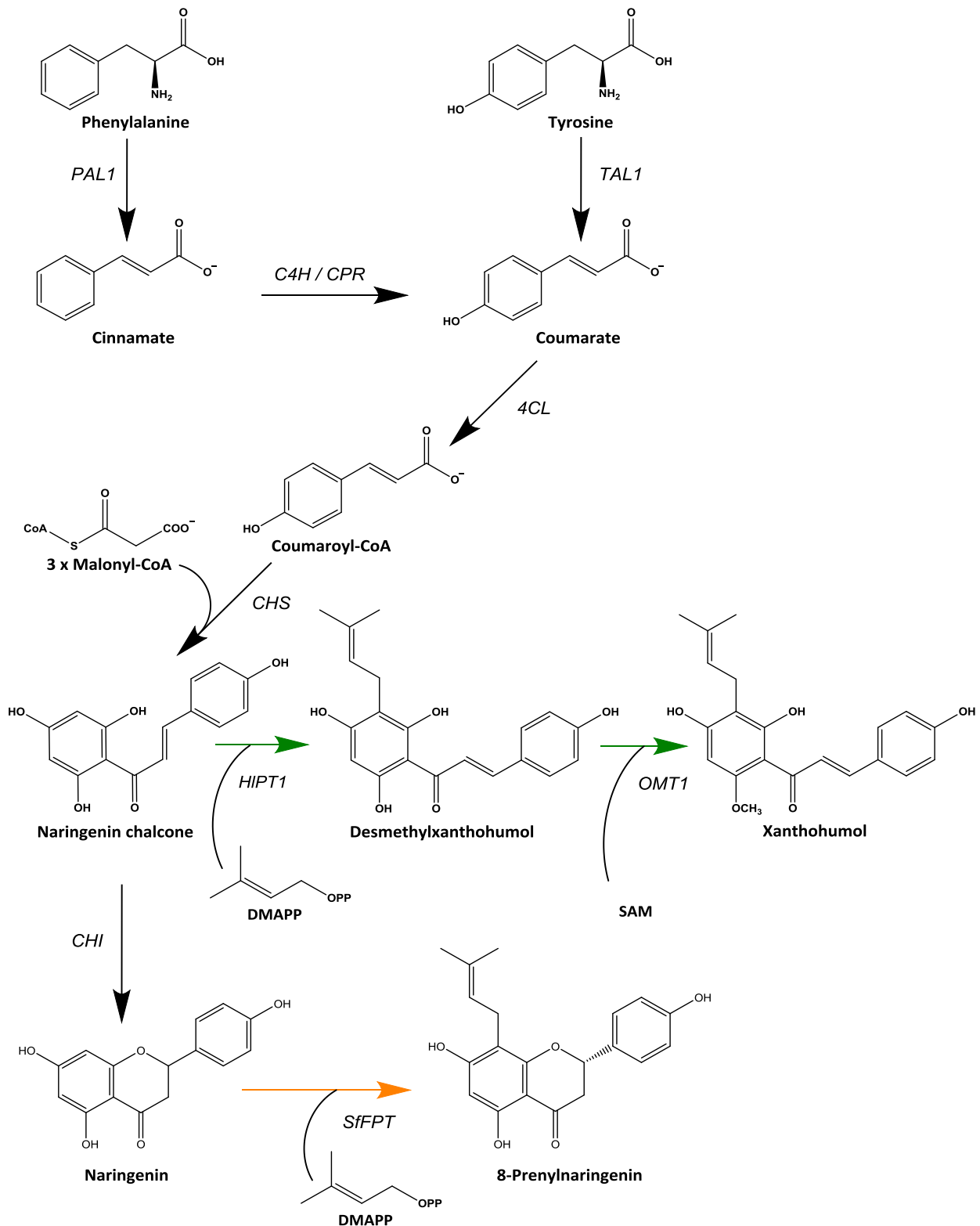


Figure 3. Engineered metabolic pathway for prenylated flavonoid biosynthesis in *S. cerevisiae*.

H. lupulus genes (green) and a *S. flavesescens* gene (orange) were overexpressed: *HIPT1* (*Humulus lupulus* prenyltransferase 1), *OMT1* (desmethylxanthohumol 6'-O-methyltransferase) and *SfFPT* (*Sophora flavesescens* prenyltransferase). Bold dark arrows indicate the engineered naringenin production pathway as described by Koopman et al. (2012): *PAL1*, phenylalanine ammonia lyase; *C4H*, Cinnamate 4-hydroxylase; *CPR1*, cytochrome P450 reductase; *4CL*, 4-coumaric acid-CoA ligase; *CHS*, chalcone synthase; *CHI1*, chalcone isomerase and *TAL1*, tyrosine ammonia lyase. DMAPP, dimethylallyl diphosphate; SAM, S-adenosyl methionine.

Results

Xanthohumol Biosynthesis

Selection of xanthohumol biosynthesis genes and *S. cerevisiae* strains

Studies have shown that the biosynthetic genes *HIPT1* and *OMT1* from *H. lupulus* are responsible for xanthohumol production (44,45). Thus these genes were selected for expression in *S. cerevisiae*, after which their coding regions were codon optimized (co) for yeast and cloned into an expression vector, pMEN1. This expression vector also harboured a truncated HMG-CoA reductase gene (*HMGRt*), which is responsible for formation of mevalonate in the isoprenoid pathway. Using a truncated version will circumvent feedback regulation on the enzyme HMG-CoA reductase through which ultimately dimethylallyl pyrophosphate (DMAPP) can be overproduced (48). Since DMAPP is essential for prenylation, and the only prenyl donor accepted by the prenyltransferase *HLPT1*, we have chosen to increase the supply of this key prenyl donor using expression of *HMGRt*.

S. cerevisiae strains for introduction of plasmid pMEN1 were two previously engineered strains: IMK393 (*aro3Δ*, *ARO4^{G226S}*, *pdc6Δ*, *pdc5Δ*, *aro10Δ*), optimized for aromatic amino acid synthesis and PATW066 (*aro3Δ*, *ARO4^{G226S}*, *pdc6Δ*, *pdc5Δ*, *aro10Δ*, *atPAL1*↑, *atcoC4H*↑, *coCPR1*↑, *atCHI1*↑, *atCHS3*↑, *coCHS3*↑, *at4CL3*↑), derived from IMK393 and engineered for naringenin biosynthesis (39, 49). Strain IMK393 was used in this experiment as a control strain as it is not able to produce naringenin chalcone, a precursor of xanthohumol. In contrary, PATW066 is capable of naringenin chalcone production.

Xanthohumol production in *S. cerevisiae* strains

Introduction of the expression vector pMEN1 into PATW066 and IMK393 resulted in strains PPF1 and PPF2, respectively. For biotransformation, cultures of PPF1 and PPF2 were inoculated in duplo into 250 ml shake-flasks containing SMG medium. Additionally, both strains were inoculated in duplo into shake-flasks containing SMG medium supplemented with naringenin chalcone. Naringenin chalcone was supplied to these cultures to provide more substrate for xanthohumol production. Finally, strain PATW066 was also inoculated in duplo into shake-flasks containing SMG medium to serve as a control for xanthohumol production and to see whether naringenin (chalcone) was produced. Yeast cultures were grown for 120 hours, after which the culture medium and cells were separated by centrifugation prior to prenylated flavonoid extraction. Culture medium and cells were separately analyzed in order to see whether xanthohumol would accumulate in the cells or would be released into the culture medium.

Xanthohumol was detected in the supernatant of PPF1 and PPF2 cultures supplied with naringenin chalcone (Fig. 4). Xanthohumol was not detected in the supernatant of PPF1 and PPF2 cultures without naringenin chalcone supplementation, nor in the control strain PATW066 (Fig. 4). Analysis of the cell pellet samples did not show any presence of xanthohumol (Data not shown). These results show that xanthohumol was produced by

expression of *HIPT1*, *OMT1* and *HMGRT* with supplementation of naringenin chalcone. Unfortunately, *de novo* production of xanthohumol has not yet been achieved.

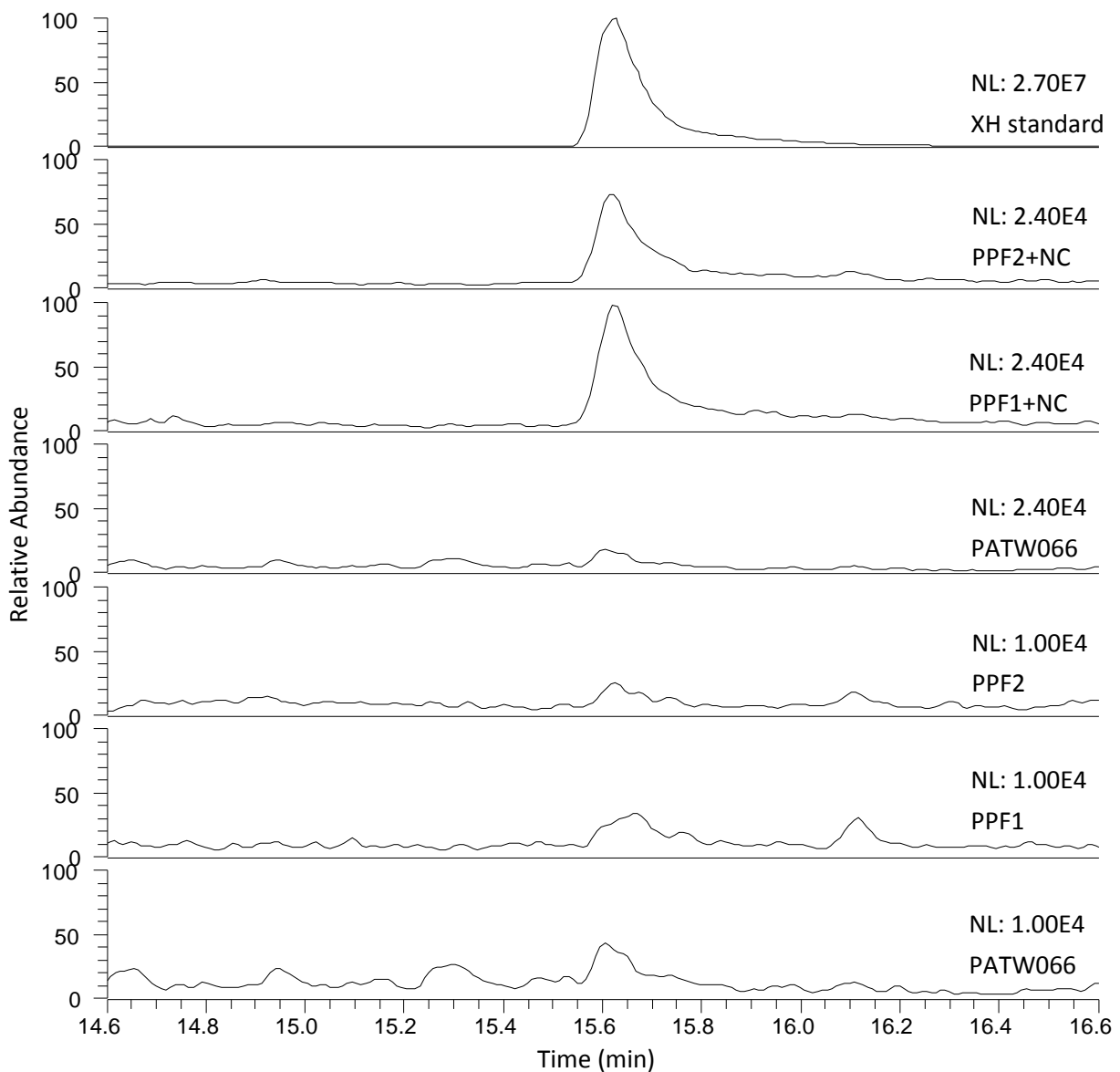


Figure 4. LC-MS analysis of xanthohumol in the supernatant of strains PPF1, PPF2 and PATW066. All strains were cultured in 50 ml SMG medium for 120 hours. Strains PPF1 and PPF2 were additionally cultured with supplementation of naringenin chalcone. The culture medium (supernatant) was separated from the cell pellet by centrifugation. The supernatant was then used for extraction with ethyl acetate and analyzed by LC-MS in negative mode. One representative of each duplo is shown. Detection of xanthohumol at retention time (RT): 15.63 min and mass (m/z): 353. Xanthohumol standard was used at 0.1 M. NC, naringenin chalcone.

8-Prenylnaringenin Biosynthesis

Selection of 8-prenylnaringenin biosynthesis genes and *S. cerevisiae* strains

Two prenyltransferases from *S. flavescens* have been identified that can prenylate naringenin at the C-8 position, *SfN8DT* and *SfFPT*, which share high (93%) sequence similarity (43). Chen et al. (2013) has shown that the enzyme *SfFPT* has a stronger affinity and higher catalytic efficiency with the prenyl acceptor naringenin and the prenyl donor DMAPP, compared to *SfN8DT*. Therefore, we have chosen to clone the coding region of *SfFPT* into an expression vector, pMEN2. As the prenyl donor DMAPP is also essential for prenylation by *SfFPT*, we also cloned *HMGRt* into pMEN2 in order to increase the supply of DMAPP. The *S. cerevisiae* strain for introduction of plasmid pMEN2 was PATW066, capable of producing naringenin, the precursor of 8-prenylnaringenin.

8-prenylnaringenin production in *S. cerevisiae*

The expression vector pMEN2 was introduced into strain PATW066, resulting in strain PPF3. Cultures of PPF3 were inoculated in duplo into 250 ml shake-flasks containing SMG medium and in duplo into 250 ml shake-flasks containing SMG medium supplemented with 250 μ M naringenin. Naringenin supplementation was performed to increase substrate levels for 8-prenylnaringenin production. Additionally, PATW066 was also inoculated in duplo into shake-flasks containing SMG medium to serve as a control for naringenin production. Yeast cultures were grown for 120 hours, after which culture medium and cells were separated by centrifugation prior to prenylated flavonoid extraction. Culture medium and cells were separately analyzed in order to see whether 8-prenylnaringenin would accumulate in the cells or would be released into the culture medium. To test whether we could further enhance the extraction of 8-prenylnaringenin from the yeast cell pellet samples, half of the pellet samples were treated with Zymolyase prior to extraction.

8-prenylnaringenin was detected in the supernatant of PPF3 cultures supplied with naringenin and in the supernatant of PPF3 cultures without naringenin supplementation (Fig. 5). Furthermore, 8-prenylnaringenin could be detected in the cell pellet of PPF3 cultures supplied with naringenin, treated and untreated with Zymolyase (Supplementary Fig. 1). 8-prenylnaringenin might also be present in the cell pellet sample of PPF3 cultures, treated with Zymolyase, although the data is not conclusive enough. No detectable amounts of this prenylated flavonoid or from 6-prenylnaringenin were seen in the supernatant and cell pellet samples of the control, and neither did we detect it in the cell pellet samples of PPF3 cultures, untreated with Zymolyase (Supplementary Fig. 1). Based on the analysis of the cell pellet samples of strain PPF3, Zymolyase treatment seems to enhance extraction of 8-prenylnaringenin. These results show that 8-prenylnaringenin was produced by expression of *SfFPT* and *HMGRt* both with and without supplementation of naringenin, indicating that *de novo* production of this prenylated flavonoid was achieved.

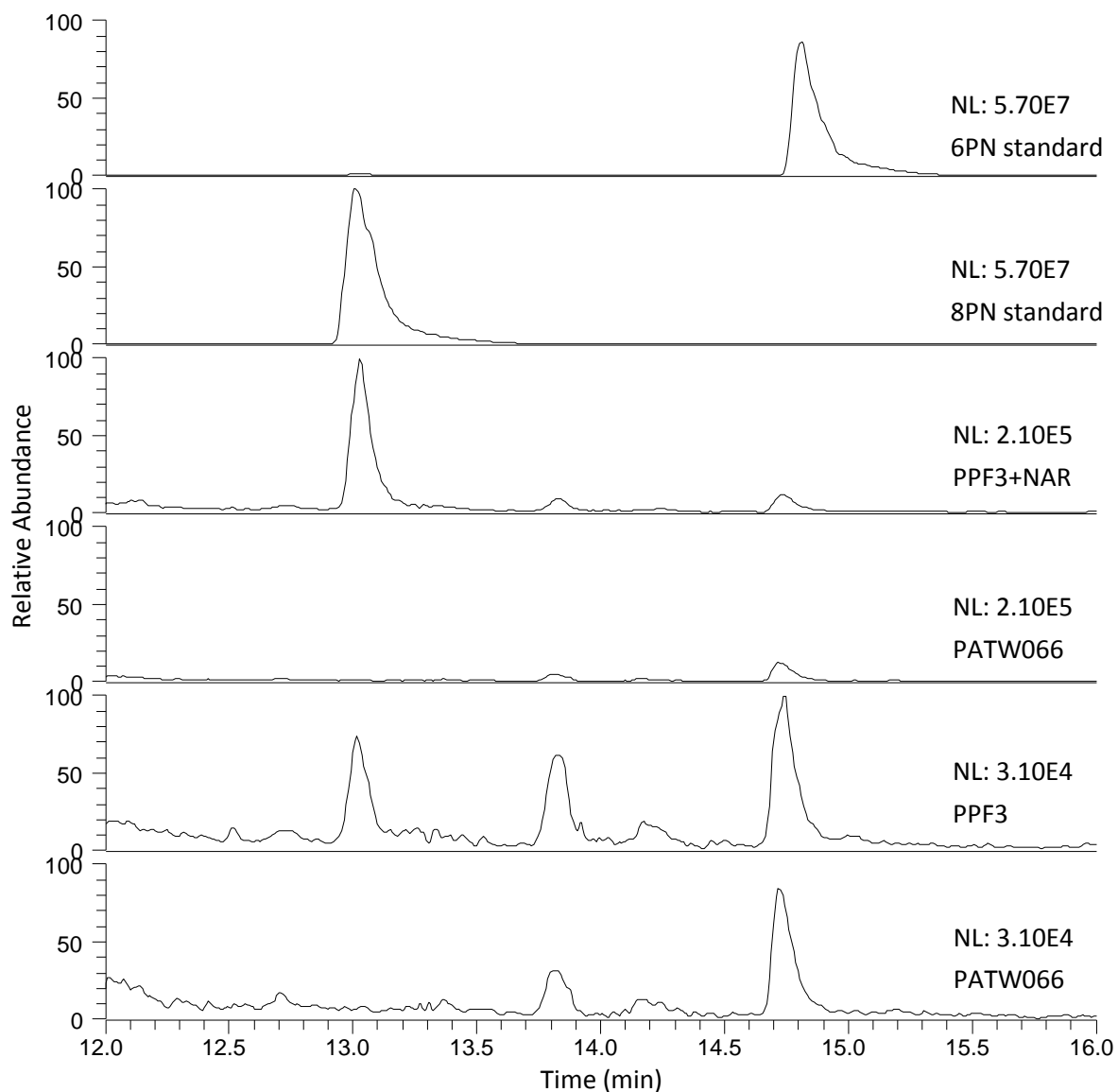


Figure 5. LC-MS analysis of 8-prenylnaringenin in the supernatant of strains PPF3 and PATW066. All strains were cultured in 50 ml SMG medium for 120 hours. Strain PPF3 was additionally cultured with supplementation of naringenin. The supernatant was separated from the cell pellet by centrifugation. The supernatant was then used for extraction with ethyl acetate and analyzed by LC-MS in negative mode. One representative of each duplo is shown. Detection of 8-prenylnaringenin at RT: 13.00 min and m/z : 339. 8-prenylnaringenin and 6-prenylnaringenin standards were used at 0.25 M. NAR, naringenin.

S. cerevisiae Strain Improvements using CRISPR-Cas9

Strain PATW066 was further metabolically engineered in order to optimize naringenin (chalcone) production. First of all, *TSC13*, encoding a very-long-chain enoyl-CoA reductase, was replaced with the homologous gene *MdECR* using CRISPR-Cas9. The enzyme encoded by *TSC13* was found to be responsible for accumulation of phloretic acid via reduction of coumaroyl-CoA (50). This accumulation leads to carbon loss in the flavonoid biosynthetic pathway and was therefore a target for strain improvement. However, as *TSC13* is also essential for fatty acid synthesis, this gene could not simply be knocked out as this would be lethal for the yeast. Therefore a different engineering approach was required. We have chosen for homologous gene replacement, as it was shown that replacement of *TSC13* by *MdECR* from apple (*Malus domestica*) resulted in a complete loss of phloretic acid production while maintaining a similar growth rate compared to the control (51).

Additionally, naringenin concentrations increased upon *TSC13* replacement in *S. cerevisiae* as well. Strain PATW066 was selected for homologous gene replacement of *TSC13* by *coMdECR* using CRISPR-Cas9. *TSC13* replacement by *coMdECR* in strain PATW066 yielded strain PATW088 (*aro3Δ*, *ARO4^{G226S}*, *pdc6Δ*, *pdc5Δ*, *aro10Δ*, *tsc13Δ*, *atPAL1*↑, *atcoC4H*↑, *coCPR1*↑, *atCHI1*↑, *atCHS3*↑, *coCHS3*↑, *at4CL3*↑, *coMdECR*).

Secondly, a yeast codon optimized tyrosine ammonia lyase (*coTAL1*) gene from *Rhodobacter capsulatus* was integrated into the *S. cerevisiae* genome. *TAL1* is responsible for conversion of tyrosine into coumarate and previous integration of the yeast codon-optimized *coTAL1* gene has shown to increase production levels of naringenin (39). Considering a target locus for integration of *coTAL1* using CRISPR-Cas9, the *SPR1* locus was chosen. The translational product of the *SPR1* gene is a β-glucosidase involved in hydrolysis of flavonoid glucosides. This function is not essential for (prenylated) flavonoid production and previous work has demonstrated that *SPR1* is also not essential for cell growth as deletion of this gene resulted in a promoted cell growth (52). Strain PATW088 was selected for integration of *coTAL1* using CRISPR-Cas9. Integration of *coTAL1* into the genome of strain PATW088 yielded strain PATW103 (*aro3Δ*, *ARO4^{G226S}*, *pdc6Δ*, *pdc5Δ*, *aro10Δ*, *tsc13Δ*, *spr1Δ*, *atPAL1*↑, *atcoC4H*↑, *coCPR1*↑, *atCHI1*↑, *atCHS3*↑, *coCHS3*↑, *at4CL3*↑, *coMdECR*, *coTAL1*↑).

Finally, deletion of the previously integrated chalcone isomerase (*atCHI1*) was attempted to provide more naringenin chalcone for xanthohumol production. The integrated *atCHI1* gene is responsible for conversion of naringenin chalcone into naringenin. However, naringenin chalcone can also spontaneously cyclize to naringenin at pH values > 6.5 (53). As these conditions are also met during flavonoid biosynthesis in *S. cerevisiae*, substrate availability of naringenin chalcone for biosynthesis of xanthohumol could become limited. In order to optimize xanthohumol production levels, *atCHI1* was targeted for gene knockout using CRISPR-Cas9. Knockout of *atCHI1* in strain PATW103 yielded strain PATW105 (*aro3Δ*, *ARO4^{G226S}*, *pdc6Δ*, *pdc5Δ*, *aro10Δ*, *tsc13Δ*, *spr1Δ*, *atPAL1*↑, *atcoC4H*↑, *coCPR1*↑, *atCHS3*↑, *coCHS3*↑, *at4CL3*↑, *coMdECR*, *coTAL1*↑). PCR confirmation on the knockout of *atCHI1* in strain PATW105 did not provide a conclusive result, however a strong yellow color formation was observed in the yeast cell pellet of PATW105. The same color formation was seen when

naringenin was converted to naringenin chalcone by addition of NaOH.

HPLC analysis, as performed by Levisson et al. (2018), of strains PATW088, PATW103 and PATW105 showed no phloretic acid production and slightly increased naringenin production levels (Data not shown). Unfortunately, naringenin chalcone could not be detected with this HPLC analysis method due to acidic conditions as formic acid was used in the eluent.

Strain PATW103 is to be tested for improved 8-prenylnaringenin production. This strain is expected to produce more naringenin than strain PATW066. An increase in naringenin production should stimulate the formation of 8-prenylnaringenin as well, thus transformation of strain PATW103 with pMEN2 should result in more 8-prenylnaringenin, compared to strain PPF3.

Strain PATW105 is to be tested for improved xanthohumol production. This strain is expected to have higher naringenin chalcone levels when compared to strain PATW066. Thus, transformation of PATW105 with pMEN1 is expected to result in higher levels of xanthohumol, compared to strains PPF1 and PPF2. Of course, the aim will be *de novo* production of xanthohumol.

Discussion

The results of this study show the possibility of a *S. cerevisiae* expression platform for production of prenylated flavonoids. Expression of naringenin biosynthetic genes, the plant flavonoid prenyltransferase *HIPT1* and the methyltransferase *OMT1* led to the production of xanthohumol. Additionally, expression of naringenin biosynthetic genes and the flavonoid prenyltransferase *SfFPT* led to the production 8-prenylnaringenin. We also report for the first time *de novo* production of 8-prenylnaringenin in *S. cerevisiae*. Previous studies have relied on supplementation of the prenyl acceptors naringenin chalcone and naringenin to the medium of transgenic yeast cultures for the production of prenylated flavonoids (42, 43). In the current study, similar results were obtained through prenyl acceptor supplementation. However, we were able to produce 8-prenylnaringenin *de novo* in *S. cerevisiae* with our current expression system.

Strains PPF1 and PPF2 were able to produce xanthohumol, however only when the cultures were supplied with naringenin chalcone (Fig. 4). From the data (Fig. 4), we can see a slightly bigger peak for xanthohumol in the supernatant of the PPF1 culture supplemented with naringenin chalcone, compared to supernatant of the PPF2 culture supplemented with naringenin chalcone. This would make sense as strain PPF2 can only produce xanthohumol from the supplied amount of naringenin chalcone. Strain PPF1, however, is able to produce more substrate for xanthohumol production. It produces naringenin, and thus naringenin chalcone which can be converted to desmethylxanthohumol and eventually to xanthohumol. Both PPF1 and PPF2 cultures without naringenin chalcone supplementation show no peak for xanthohumol, possibly due to a lack of substrate availability.

The prenylated flavonoid was found to be secreted into the culture medium, as the cell pellets did not show any presence of xanthohumol. This study is the first to report that xanthohumol is secreted upon production in engineered *S. cerevisiae*. In previous studies, following the fate of xanthohumol during the brewing process, they found that xanthohumol can be adsorbed to the cell wall of *Saccharomyces pastorianus* (54, 55). Assuming that xanthohumol would also be absorbed to the cell wall of PPF1 and PPF2 cultures, we would expect to see xanthohumol in the yeast cell pellet. However, as we cannot identify xanthohumol in the cell pellets, this adsorption process might not be efficient enough. Treatment of the cell pellet with Zymolyase could reveal whether xanthohumol was extracted efficiently from the cell pellet samples in our study. It now remains to be elucidated whether xanthohumol is entirely secreted into the culture medium and does not accumulate on the cell wall or whether the adsorption of xanthohumol might be concentration dependent. Another explanation for not finding xanthohumol in the cell pellet is that *S. cerevisiae* simply does not display the same xanthohumol adsorbing effect as *S. pastorianus*.

With our current yeast expression system we are only able to produce xanthohumol through prenyl acceptor supplementation. However, even with substrate supplementation, only small traces of xanthohumol were found in the supernatant samples. The current method of supplementation with naringenin chalcone might not be efficient enough for production of xanthohumol, considering that the spontaneous cyclization of naringenin chalcone towards naringenin continues under neutral and basic conditions (pH values > 6.5) (53). Naringenin chalcone is added to the culture medium under basic conditions and remains under neutral conditions within the yeast cell. These conditions would suggest conversion of naringenin chalcone towards naringenin, and thus a decrease in substrate availability for xanthohumol production. We could observe slightly increased peaks for naringenin in the supernatant samples of cultures PPF1 and PPF2, supplied with naringenin chalcone, when compared with the supernatant sample of the PPF1 culture without supplementation. Although this data is not quantitative, we could argue that in this case the supplied naringenin chalcone was partially converted into naringenin, resulting in a decreased desmethylxanthohumol and xanthohumol formation. Future studies would need to take into account the partial conversion of the prenyl acceptor, when using supplementation of naringenin chalcone.

From previous studies, it is known that both xanthohumol and desmethylxanthohumol can partially isomerize towards isoxanthohumol and 6/8-prenylnaringenin, respectively (28, 45, 56). This partial conversion occurs at increased temperatures, e.g. during the boiling of wort. Additionally, basic conditions have been found to affect the isomerization of xanthohumol and desmethylxanthohumol, having a faster conversion rate with increasing pH (55). As our yeast cultures do not experience a boiling process, a conversion is not suspected to happen. Also, during growth, the yeast culture medium becomes more acidic. Therefore we do not expect the presence of isoxanthohumol and 6/8-prenylnaringenin in the cultures of PPF1 and PPF2. To confirm this, we checked the LC-MS data for peaks of 6-prenylnaringenin and 8-prenylnaringenin, which were used as standards during the measurements. Unfortunately, isoxanthohumol was not used as a standard and could therefore not be searched for. No peaks of 6-prenylnaringenin or 8-prenylnaringenin were found in the supernatant or pellet samples of PPF1 and PPF2. This result partially confirms our theory that we do not expect isomerization to occur during prenylated flavonoid production in our yeast cultures. The LC-MS data was checked for desmethylxanthohumol, but no peaks were found in the supernatant or pellet samples of PPF1 and PPF2. This could indicate that the intermediate compound desmethylxanthohumol is being methylated efficiently and thus not found in our samples.

Another important factor influencing the production of xanthohumol is the availability of the prenyl donor DMAPP. As DMAPP is essential for prenylation, the available amount of this prenyl donor could become a limiting factor for prenylation of naringenin chalcone. By expression of a truncated HMG-CoA reductase in the PPF1 and PPF2 yeast cultures, formation of DMAPP in the isoprenoid pathway should have been increased. Although we

did not measure for an increased production of DMAPP, we can suggest that the amount of the prenyl donor is still not enough for efficient bioconversion from naringenin chalcone to desmethylxanthohumol. A previous study had shown that the bioconversion of 8-prenylnaringenin from naringenin was increased 44-fold by a site mutation in the *ERG20* gene encoding farnesyl diphosphate synthase (FPPS) (57). The mutation of FPPS resulted in a decreased conversion of DMAPP towards farnesyl diphosphate, the building block for ergosterol in yeast. This result suggests that increasing the availability of the prenyl donor may indeed be a good strategy for production of prenylated flavonoids. Further studies are needed to confirm whether the mutation of FPPS would also result in an increased bioconversion from naringenin chalcone to xanthohumol. It might also be worth to combine several strategies for an increase in DMAPP availability in order to optimize the prenylation reactions. Other strategies used by Brown et al. (2015) to increase DMAPP formation were installing a second copy of *IDI1*, encoding isopentenyl pyrophosphate (IPP) isomerase for DMAPP formation, and installing a second copy of *MAF1* which directs IPP away from tRNA biosynthesis. These strategies and the mutation of FPPS could also be applied to our work to further increase DMAPP formation. In this way, prenyl donor availability could become a less limiting factor in prenylated flavonoid production.

Within our yeast expression system, we decided to express a yeast codon optimized *HIPT1*. The N-terminus of this protein contains a transit peptide sequence for targeting to the chloroplast. However, expression of full-length *HIPT1* could result in a lowered enzymatic activity due to possible hindrance by the N-terminal signal peptide. A lowered enzymatic activity was found for *Lupinus albus prenyltransferase 1 (LaPT1)*. Expression of *LaPT1* in yeast without the transit peptide sequence increased the overall activity of the protein, but the drawback is that it also increased the K_m value significantly (58). Interestingly, several full length proteins of prenyltransferases have been found to possess nearly the same activity as their truncated forms, in which the transit peptide sequences were completely removed (59, 60). It remains largely unknown what the exact hindering effect of the transit peptides is on the enzymatic activity of flavonoid prenyltransferases.

So far, no attempts have been made to express a truncated version of *HIPT1* in *S. cerevisiae*. Therefore, it will be worth testing whether a truncated *HIPT1* increases the overall enzymatic activity and thus xanthohumol production.

Recently, another aromatic prenyltransferase, *Humulus lupulus prenyltransferase 1-like (HIPT1L)*, has been functionally identified from hop glandular trichomes (57). This gene shares a sequence identity of 98.5% with *HIPT1*, therefore labelled as HLPT1-like. Expression of *CCL1*, *CHS_H1* and *Arabidopsis* codon-optimized *PT1L* in *S. cerevisiae*, fed with coumarate, led to the production of desmethylxanthohumol, indicating the presence of another prenyltransferase capable of prenylating naringenin chalcone (61). Interestingly, Ban et al. (2018) managed to boost desmethylxanthohumol production through co-expression of *Arabidopsis* codon-optimized *PT1L* and a type IV CHI. The CHI family can be classified into four subfamilies (type I to IV), of which type III and IV do not possess CHI activity. Therefore

these types are renamed to CHI-like proteins (CHIL). Expression of both *PT1L* and *CHIL2*, a type IV CHI, in *S. cerevisiae* resulted in a 2.3 fold increase in desmethylxanthohumol production. Not only did *CHIL2* increase the production of desmethylxanthohumol, but it also enhanced the activity of the expressed chalcone synthase (CHS), thereby showing an increase in naringenin levels. These results demonstrated a key role for *CHIL2* in desmethylxanthohumol and xanthohumol production through protein-protein interactions with *PT1L* and *CHIL2*. Ban et al. (2018) showed that an active desmethylxanthohumol biosynthetic metabolon is formed by CHS, *PT1L* and *CHIL2* that can efficiently produce prenylchalcones. Future studies have to assess whether expression of *CHIL2* and *HIPT1* in *S. cerevisiae* would also result in an increased production of desmethylxanthohumol. Additionally, *CHIL2* should be tested for interaction with *CHS3*, the CHS used in our yeast expression system, as Ban et al. (2018) expressed a different CHS, namely *CHS_H1* from hops. It would be interesting to see if *CHIL2* can apply the same protein-protein interactions when expressed with *HIPT1* and *CHS3* and thereby increase both naringenin and desmethylxanthohumol production.

Strain PPF3 was able to produce 8-prenylnaringenin with and without supplementation of the prenyl acceptor naringenin (Fig. 5). As expected, we see more 8-prenylnaringenin in the cultures that were supplied with naringenin. This prenylated flavonoid could be seen in both the culture medium and in the cell pellets of strain PPF3 (Fig. 5 and Supplementary Fig. 1). However, most of the 8-prenylnaringenin is secreted into the culture medium as we can see smaller peaks for this compound in the cell pellets. This characteristic of secretion into the medium was also seen for xanthohumol, possibly applying to all prenylated flavonoids. Interestingly, we could observe 8-prenylnaringenin in the cell pellet of *S. cerevisiae* samples treated with Zymolyase, whereas untreated samples did not show any presence of the prenylated flavonoid. This finding is in contrast to previous work, where 8-prenylnaringenin could not be detected in yeast cells treated with Zymolyase, but only in the culture medium (42). One possible explanation for our finding might be that we expressed *SfFPT*, whereas Sasaki et al. (2009) used expression of the paralogue *SfN8DT-1*. It is clear that more attention is needed for localization of the produced prenylated flavonoids, which will greatly enhance extraction of these compounds. By making a *SfFPT*-GFP fusion protein, we could gain more insight into where this protein is localized inside the yeast cell. In turn, this information will provide us with a more clear view of where 8-prenylnaringenin is produced and possibly retained.

To see the specificity of prenylation by *SfFPT*, we also looked for 6-prenylnaringenin in the samples of strains PATW066 and PPF3. 6-prenylnaringenin was not found in any of the samples of strain PPF3, indicating that the prenylation reaction by *SfFPT* is specific for the C-8 position (Fig. 5 and Supplementary Fig. 1). This strong regiospecificity of *SfFPT* is also consistent with previous work (43).

We were able to produce 8-prenylnaringenin both with and without supplementation of the prenyl acceptor naringenin. However, *de novo* production still shows only trace amounts of

the prenylated flavonoid. As mentioned earlier, prenylation reactions are highly dependent on the availability of the prenyl donor DMAPP. So in order to boost production levels of 8-prenylnaringenin, the levels of DMAPP should be increased as well. Clearly, the strategy of expressing *HMGRT* is not enough and therefore we propose to also apply the strategies mentioned before for boosting the availability of the prenyl acceptor DMAPP.

As the substrate availability for both xanthohumol and 8-prenylnaringenin production is also limiting, we metabolically engineered strain PATW066 to increase the formation of both naringenin chalcone and naringenin. Successful replacement of *TSC13* by the homologous gene *MdECR* resulted in strain PATW088. This strain showed a complete loss of phloretic acid production, consistent with previous work (51).

Further engineering of strain PATW088 was performed by integration of *coTAL1*, resulting in strain PATW103. Expression of *coTAL1* in strain PATW103 should result in a conversion of tyrosine into coumarate, a precursor of naringenin (chalcone). Thus a further increase in naringenin production is expected to be seen in PATW103. HPLC-analysis revealed a slight increase in naringenin production in strain PATW103, compared to strain PATW066. Unfortunately, we had expected to see a sharper increase in the naringenin levels through these strain improvements. A possible explanation for the unsatisfying results might be that our HPLC-analysis was inaccurate and needs to be repeated. The cultures of each strain were inoculated only once, instead of making duplicates. The analysis on strains PATW088 and PATW103 needs to be repeated with more replicates to be certain of an increase in naringenin production. Additionally, to gain more insight into the production of naringenin over time, samples can be taken at certain time points from 50 ml yeast cultures of PATW088 and PATW103.

In order to increase the production of xanthohumol, substrate levels of naringenin chalcone should be increased as well. Since naringenin chalcone is converted into naringenin by *CHI1* and spontaneous isomerization, *TSC13* gene replacement and *coTAL1* integration are not sufficient to generate an increase in xanthohumol production. Therefore, *CHI1* was targeted for gene knockout. The resulting strain, PATW105, could not be confirmed for successful gene knockout as every PCR failed to show bands. However, when growing strain PATW105 on plate and in culture medium, we could observe a strong yellow color formation. This color formation would indicate the presence of naringenin chalcone. HPLC analysis was performed with strain PATW105 as well, to confirm the presence of naringenin chalcone and thus successful gene knockout of *CHI1*. Unfortunately, naringenin chalcone was detected neither in strain PATW105 nor in the used standard. Most likely, our analysis method was inappropriate for measuring naringenin chalcone due to the formic acid used in the eluent, which converts the naringenin chalcone. Nevertheless, we are convinced that we have successfully deleted *CHI1* in strain PATW105, but future studies are needed for confirmation. The engineered strains PATW103 and PATW105 could be used for introduction of the plasmids pMEN2 and pMEN1, respectively. Introduction of pMEN2 into PATW103 should result in increased *de novo* 8-prenylnaringenin production, since the resulting strain

produces more of the substrate naringenin compared to PFF3. Introduction of pMEN1 into PATW105 should show an increase in the production of xanthohumol when comparing to PPF1. This strategy may also result in *de novo* production of xanthohumol, which has not yet been achieved in *S. cerevisiae*.

Conclusion

Here we provide a report on the production of the prenylated flavonoids xanthohumol and 8-prenylnaringenin using *S. cerevisiae*. Metabolic engineering of *S. cerevisiae* by expressing *PAL*, *TAL*, *C4H*, *CPR*, *4CL*, *CHS*, *CHI*, *SfFPT* and *HMGRt* resulted in *de novo* production of 8-prenylnaringenin, not yet achieved before. Because *de novo* production of xanthohumol was not achieved and *de novo* production of 8-prenylnaringenin showed only relatively small peaks, improvements are required to enhance the production efficiency of both prenylated flavonoids. Several bottlenecks have been discussed in this study regarding optimization of both naringenin (chalcone) and prenylated flavonoid production. However, not only flux optimization should be focused upon, but also localization studies need attention in order to gain more insight into (prenyated) flavonoid biosynthesis in *S. cerevisiae*. These insights could in turn help simplify extraction of prenylated flavonoids. Future attempts on tackling the addressed issues should result in an increased production efficiency for both xanthohumol and 8-prenylnaringenin.

The currently engineered yeast strains serve as a starting platform for the production of prenylated flavonoids which can be used as food preservatives, pharmaceuticals and nutraceuticals.

Methods

Strains and Cultivation Conditions

The *S. cerevisiae* strains that were used in this study are listed in Table 2. They are all derived from the IMK393 yeast strain, which in turn was derived from the CEN.PK2-1c yeast strain containing four auxotrophies (62). The IMK393 strain was metabolically engineered to alleviate feedback inhibition of aromatic amino acid biosynthesis (39). *S. cerevisiae* cultures were grown at 30 °C at 300 rpm in 250 ml shake flasks containing 50 ml synthetic medium (demineralized water, 6.8 g/L yeast nitrogen base without amino acids) and 20 g/L glucose (SMG). For each strain, the media was supplemented with required auxotrophic markers (20 mg/L histidine, 120 mg/L leucine, 20 mg/L tryptophan and 20 mg/L uracil).

E. coli strain DH5 α was used as a host for transformation and amplification of plasmids. DH5 α electrocompetent cells (Thermo Scientific) were grown at 37 °C at 250 rpm in Luria Broth (LB) medium. 100 μ g/L ampicillin was added to the LB medium for transformation and amplification of plasmids containing an ampicillin resistance marker.

Molecular Biology Procedures

PCR amplification was performed using either Q5[®] High-Fidelity DNA Polymerase or Phusion[®] High-Fidelity DNA Polymerase (New England Biolabs) according to the manufacturer's instructions on a Mastercycler[®] nexus GX2 (Eppendorf). Separation of PCR fragments was performed using a 1% (w/v) agarose gel in 1x TAE buffer (40 mM Tris-acetate pH 8.0 and 1mM EDTA). Gel purification of PCR products was performed using NucleoSpin[®] Gel and PCR Clean-up kit (Macherey-Nagel). DNA isolation from *S. cerevisiae* was performed as previously described (63). Transformation and amplification of plasmids were performed with *E. coli* DH5 α electrocompetent cells according to the manufacturer's instruction. Isolation of plasmids from transformed *E. coli* cells was performed with the NucleoSpin[®] Plasmid EasyPure kit. Sequencing of constructs was performed by Macrogen (Macrogen Europe, Amsterdam, The Netherlands).

Plasmid and Strain Construction

All plasmids used in this study are listed in Table 1. The plasmids were constructed by *in vivo* assembly as described previously (64). The xanthohumol biosynthesis genes, *HIPT1* (GenBank accession AB543053) and *OMT1* (GenBank accession ABZ89565), and the 8-prenylnaringenin biosynthesis gene, *SfFPT* (GenBank accession KC513505), were synthesized by Integrated DNA Technologies, BVBA (Leuven, Belgium). These genes were codon optimized for *S. cerevisiae* using the Jcat algorithm (65). The biosynthesis genes were flanked by different promoter and terminator combinations to avoid plasmid instability due to homologous recombination. For plasmid construction, each fragment contained at least 60 bp of flanking regions to promote *in vivo* assembly.

Construction of pMEN1 required assembly of eight separate fragments. Fragment HIPT was constructed using primer pair MvdH2/MvdH3 on the synthetic HIPT1 gene. Fragment PGK1t-2 μ -TEF1p was constructed using primer pair MvdH4/MvdH5 on pCPW002. Fragment HMGRt was constructed using primer pair MvdH6/MvdH7 on the synthetic *HMGRt* gene. Fragment CYC1t-O-PGIp was constructed using primer pair MvdH8/MvdH9 on pCPW002. Fragment OMT1 was constructed using primer pair MvdH10/MvdH11 on the synthetic OMT1 gene. Fragment ADH1t-AmpR-A was constructed using primer pair MvdH12/MM20R on pCPW002. Fragment A-TRP1-N was constructed using primer pair ML0075/MH13 on pCPW002. Fragment N-TPIp was constructed using primer pair MM9F/MvdH1 on pCPW002 (Supplementary Fig. 4).

Construction of pMEN2 required assembly of five separate fragments. Fragment HMGRt2 was constructed using primer pair MvdH6/MH14 on the synthetic *HMGRt* gene. Fragment TEF1t-AmpR-2 μ was constructed using primer pair MH15/ML0009 on pUDE188. Fragment 2 μ -HIS3-CYC1t was constructed using primer pair ML0010/MH18 on pUDE188. Fragment SffPT was constructed using primer pair MH19/MH16 on the synthetic *SffPT* gene. Fragment GAPp-TEF1p was constructed using primer pair MH17/MvdH5 on pUDE188 (Supplementary Fig. 5).

Strain PATW066 was previously constructed by integration of naringenin biosynthesis genes *atCHI1*, *atCHS3*, *at4CL3*, *atPAL1*, *coC4H*, *coCPR1* and *coCHS3* in strain IMK393 using CRISPR-Cas9 (49). Transformation of PATW066 and IMK393 with pMEN1 using the standard lithium acetate method resulted in respectively, strain PPF1 and PPF2 (66). Transformation of PATW066 and IMK393 with pMEN2 using the same method resulted in respectively, strain PPF3 and PPF4.

The PATW083 yeast strain was constructed by transforming PATW066 with plasmid p414-TEF1p-Cas9-CYC1t (67). Strain PATW083 was used for strain engineering with gRNA expression vectors and integration genes as previously described (67).

Yeast transformants were selected by plating yeast cells on selective agar plates (SMG with histidine and leucine, SMG with histidine, leucine and uracil, SMG with leucine, tryptophan and uracil or SMG with histidine, leucine, tryptophan and uracil) and confirmed by PCR using verification primers.

Table 1

Plasmids used in this study

Plasmid	Relevant genotype	Source
pCPW002	2 μ m ori, <i>TRP1</i> , P _{GAP-<i>atF3H</i>} -T _{TEF} , P _{TPI-<i>atANS</i>} -T _{PGK1} , P _{TEF1-<i>ghDFR</i>} -T _{CYC1} , P _{PGI-<i>at3GT</i>} -T _{ADH1}	Levisson et al. (2018)
pUDE188	2 μ m ori, <i>HIS3</i> , P _{TEF-<i>coCHS3</i>} -T _{TEF} , P _{GAP-<i>coCHS3</i>} -T _{CYC1}	Department of Plant Physiology at Wageningen University
pMEN1	2 μ m ori, <i>TRP1</i> , P _{TPI-<i>coHIPT1</i>} -T _{PGK1} , P _{TEF-<i>HMGRt</i>} -T _{CYC1} , P _{PGI-<i>coOMT1</i>} -T _{ADH1}	This study
pMEN2	2 μ m ori, <i>HIS3</i> , P _{TEF-<i>HMGRt</i>} -T _{TEF} , P _{GAP-<i>coSffPT</i>} -T _{CYC1}	This study
p414-TEF1p-Cas9-CYC1t	CEN/ARS, <i>TRP1</i> , P _{TEF-<i>Cas9</i>} -T _{CYC1}	DiCarlo et al. (2013)
p426-SNR52p-gRNA.TSC13.Y-SUP4t	gRNA expression vector, 2 μ m ori, <i>URA3</i> , P _{SNR52-<i>gRNA.TSC13</i>} -T _{SUP4}	Levisson et al. (2018)
p426-SNR52p-gRNA.SPR1.Y-SUP4t	gRNA expression vector, 2 μ m ori, <i>URA3</i> , P _{SNR52-<i>gRNA.SPR1</i>} -T _{SUP4}	Levisson et al. (2018)
p426-SNR52p-gRNA.CHI.Y-SUP4t	gRNA expression vector, 2 μ m ori, <i>URA3</i> , P _{SNR52-<i>gRNA.CHI</i>} -T _{SUP4}	This study

* *co*: codon optimized, *at*: *A.thaliana*.

Table 2

Strains used in this study

Strain	Relevant genotype	Source
CEN.PK2-1c	MATalpha <i>ura3 his3 leu2 trp1 MAL2-8cSUC2</i>	Entian and Kötter (2007)
IMK393	MATalpha <i>ura3 his3 leu2 trp1 MAL2-8cSUC2 Δaro3(46,1065)::loxP ARO4^{G226S} pdc6Δ(-6,-2)::loxP pdc5Δ(-6,-2)::loxP aro10Δ(-6,-2)::loxP</i>	Koopman et al. (2012)
PATW066	IMK393 <i>X-2b::P_{TDH3}-atCHI1-T_{CYC1}, P_{TPI}-atCHS3-T_{ADH1}, P_{TEF}-at4CL3-T_{TEF} XII-2b::P_{TDH3}-coPAL1-T_{CYC1}, P_{TPI}-coC4H-T_{ADH1}, P_{PGI}-coCPR1-T_{PGI}, P_{TEF}-coCHS3-T_{TEF}</i>	Levisson et al. (2018)
PATW080	PATW066 <i>can1Δ::P_{GAP1}-coF3H-T_{TEF}, P_{TPI1}-coANS-T_{PGK1}, T_{TEF}-coGhDFR-T_{CYC1}, P_{PGI1}-co3GT-T_{ADH1} exg1Δ::P_{TEF}-coCHS3-T_{TEF} spr1Δ::P_{TDH3}-coTAL1-T_{CYC1}</i>	Levisson et al. (2018)
PATW083	PATW066 p414-Cas9	This study
PATW088	PATW066 <i>tsc13Δ::coMdECR</i>	This study
PATW089	PATW083 <i>tsc13Δ::coMdECR</i>	This study
PATW103	PATW088 <i>spr1Δ::coTAL1</i>	This study
PATW104	PATW089 <i>spr1Δ::coTAL1</i>	This study
PATW105	PATW103 <i>chiΔ</i>	This study
PPF1	PATW066 pMEN1	This study
PPF2	IMK393 pMEN1	This study
PPF3	PATW066 pMEN2	This study
PPF4	IMK393 pMEN2	This study

Strain Engineering using CRISPR-Cas9

Gene fragment integration and gene knock-out was performed by using gRNA expression plasmids and homologous recombination fragments together with the yeast strain PATW083, containing the Cas9 plasmid, as described previously (67). The gRNA expression plasmids each have their own genomic targeting sequence (GTS) for the different genes to be targeted, selected by using either the Yeaststriction webtool or the ATUM gRNA Design Tool (68, 69).

Construction of gRNA expression plasmid p426-SNR52p-gRNA.CHI.Y-SUP4t required assembly of two separate fragments. Fragment 2 μ -AmpR-SNR52p-CHI-GTS was constructed using primer pair ML0009/MH23 on the gRNA expression plasmid p426-SNR52p-gRNA.TSC13.Y-SUP4t. Fragment CHI-GTS-SUP4t-URA3-2 μ was constructed using primer pair ML0010/MH22 on the gRNA expression plasmid p426-SNR52p-gRNA.TSC13.Y-SUP4t.

The plasmids were isolated after *in vivo* assembly in *S. cerevisiae* and retransformed to *E. coli* via electroporation. Transformants were selected on LB agar plates containing ampicillin. Subsequently, single colonies of *E. coli* transformants were grown in 5 ml LB medium containing ampicillin, after which plasmids were isolated from these cultures. The isolated plasmids were then checked by PCR and sequencing.

The integration gene *coMdECR* was available at the Department of Plant Physiology at Wageningen University, while *coTAL1* was obtained by a PCR amplification of genomic DNA from PATW080 using the primer set ML0017/CP171. The resulting PCR product was then used as a template for a subsequent PCR amplification using primers CP169/CP190, yielding the full length *coTAL1* integration gene. The homologous recombination repair fragment for construction of a *CHI* knockout strain was amplified from genomic DNA of PATW080 using the primer sets MH24/MH25 and MH26/27. The resulting PCR products were then used as a template for a subsequent PCR amplification using primers MH24/MH27, giving the homologous recombination fragment *ADH1t-X-2bdown*.

Each integration fragment consisted of two 60 bp flanking regions, which are upstream and downstream of the GTS and thereby deleting more than 300 bp of the target sequence during recombination.

Transformation of PATW083 with gRNA expression plasmid p426-SNR52p-gRNA.TSC13.Y-SUP4t and integration fragment *coMdECR* yielded strain PATW089. Before each next integration, the gRNA plasmid was removed from the transformed strain and before culturing experiments, both gRNA and Cas9 plasmids were removed from the transformed yeast strains. Removal of the plasmids was done by growing the transformed strain on liquid rich medium, plating on non-selective medium and subsequently confirming plasmid removal by restreaking the same colony on selective and non-selective medium. Removal of the Cas9 plasmid from strain PATW089 resulted in strain PATW088.

Subsequent transformation of PATW089 with p426-SNR52p-gRNA.SPR1.Y-SUP4t and integration fragment *coTAL1* yielded strain PATW104. Removal of the Cas9 plasmid from strain PATW104 resulted in strain PATW103.

Transformation of PATW104 with p426-SNR52p-gRNA.CHI.Y-SUP4t and the homologous recombination fragment *ADH1t-X-2bdown* and subsequent removal of both the gRNA and Cas9 plasmid yielded strain PATW105.

Analytical Methods

Xanthohumol production in shake flasks

Strain PPF1 and PPF2 were inoculated as precultures into 10 ml of SMG medium with the required auxotrophic markers histidine, leucine and uracil. The optical density of the precultures was measured at 600 nm (OD_{600}) using an Ultrospec™ 10 Cell Density Meter (Amersham Biosciences). For xanthohumol production in 250 ml shake-flasks, 50 ml of SMG medium with auxotrophic markers, histidine, leucine and uracil, was inoculated with precultures of PPF1 and PPF2 at an OD_{600} of 0.173. Two shake-flasks, inoculated with PPF1 cultures were also supplemented with naringenin chalcone. In the same way, two shake-flasks with PPF2 cultures were supplemented with naringenin chalcone. Naringenin, from a stock solution, was converted into its open ring structure naringenin chalcone by addition of NaOH and subsequently added to the yeast cultures to a final concentration of 250 μ M. Additionally, 50 ml of SMG medium with the auxotrophic markers, histidine, leucine, tryptophan and uracil, was inoculated in duplo with PATW066 at an OD_{600} of 0.173. Yeast cultures were harvested after 120 hours of growth, after which the supernatant and cell pellet were separated via centrifugation. The cell pellet and the supernatant samples were freeze-dried and afterwards extraction was performed on both samples using one time 5 ml ethyl acetate per sample. The ethyl acetate soluble portions were collected separately and evaporated to dryness. To examine the presence of flavonoids and prenylated flavonoids, the ethyl acetate extracts were dissolved in 500 μ l of 100% ethanol.

8-prenylnaringenin production in shake flasks

Strain PPF3 was inoculated as preculture into 10 ml SMG medium with the required auxotrophic markers leucine, tryptophan and uracil. For 8-prenylnaringenin production in 250 ml shake-flasks, 50 ml of SMG medium with auxotrophic markers, leucine, tryptophan and uracil, was inoculated with the preculture of PPF3 at an OD_{600} of 0.200. Two shake-flasks, inoculated with PPF3 cultures were also supplemented with naringenin. Naringenin, from a stock solution, was added to the yeast cultures to a final concentration of 250 μ M. Additionally, 50 ml of SMG medium with the auxotrophic markers, histidine, leucine, tryptophan and uracil, was inoculated in duplo with PATW066 at an OD_{600} of 0.200. Yeast cultures were harvested after 120 hours of growth, after which the supernatant and cell pellet were separated via centrifugation. Half of the cell pellet samples were treated with Zymolyase 100T (5 μ l) (Irvine, United States of America) before freeze-drying in order to enhance yeast cell lysis. The supernatant samples were not freeze-dried, but stored at -20°C after separation from the cell pellet. Afterwards, extraction was performed using two times 10 ml ethyl acetate per sample for both the cell pellet and supernatant samples. The ethyl

acetate soluble portions were collected separately and evaporated to dryness. To examine the presence of flavonoids and prenylated flavonoids, the ethyl acetate extracts were dissolved in 500 μ l of 100% ethanol.

RP-UHPLC-UV-MS analysis

Composition analysis of the ethanol extracts was performed on an Accela ultra high performance liquid chromatography (RP-UHPLC) system (Thermo Scientific, San Jose, CA, USA) equipped with a pump, autosampler and photodiode array (PDA) detector.

Samples (1 μ l) were injected onto an Acquity UPLC BEH RP18 column (2.1 mm i.d. x 150 mm, 1.7 μ m particle size) with an Acquity UPLC RP18 Vanguard guard-column (2.1 mm i.d. x 5 mm, 1.7 μ m particle size; Waters, Milford, MA, USA). Water containing 0.1% (v/v) formic acid (FA) and 1% (v/v) acetonitrile (ACN), eluent A, and ACN containing 0.1% (v/v) FA, eluent B, were used as solvents at a flow rate of 300 μ l/min. Column temperature was set at 35 °C and the PDA detector was set to measure from 200-600 nm. The following elution profile was used: 0-1.5 min, isocratic on 5% (v/v) B; 1.5-20 min, linear gradient from 5-100% B; 20-25 min, isocratic on 100% B; 25-26 min, linear gradient from 100-5% B.

Mass spectrometric (MS) analysis was performed on a LTQ Velos (Thermo Scientific) equipped with a heated ESI probe coupled to the RP-UHPLC. Spectra were acquired over an m/z (mass to charge ratio) range of 150-1500 Da in negative mode (NI). Data-dependent MS analysis was performed on the most intense (product) ion with a normalized collision energy of 35%. A dynamic mass exclusion approach was used, in which a compound detected five times within 10 s as most intense was subsequently excluded for the following 10 s, allowing data dependent MS² of less abundant co-eluting compounds. The system was tuned with genistein via automatic tuning using Tune Plus (Xcalibur 2.1, Thermo Scientific). Nitrogen was used as sheath and auxiliary gas. The ITT temperature was 400 °C and the source voltage was 3.50 kV (NI) or 4.50 kV (PI).

Standard solutions (0.1 mg/ml in EtOH) of phenolic compounds (e.i. naringenin, 8-prenylnaringenin and 6-prenynaringenin, purchased from Sigma) were used for identification by means of Xcalibur (v.2.2, Thermo Scientific).

Acknowledgements

I would like to thank my supervisors, Mark Levisson and Jules Beekwilder for their guidance and support throughout my thesis research. Of course I am also grateful for the support of the Bioscience Group and the Plant Physiology Department of Wageningen University both inside and outside the lab environment.

Additionally, I would like to thank Carla Araya-Cloutier and Jean-Paul Vincken of the Laboratory of Food Chemistry for their guidance and their contribution to my project by performing the LC-MS analysis of all our samples.

References

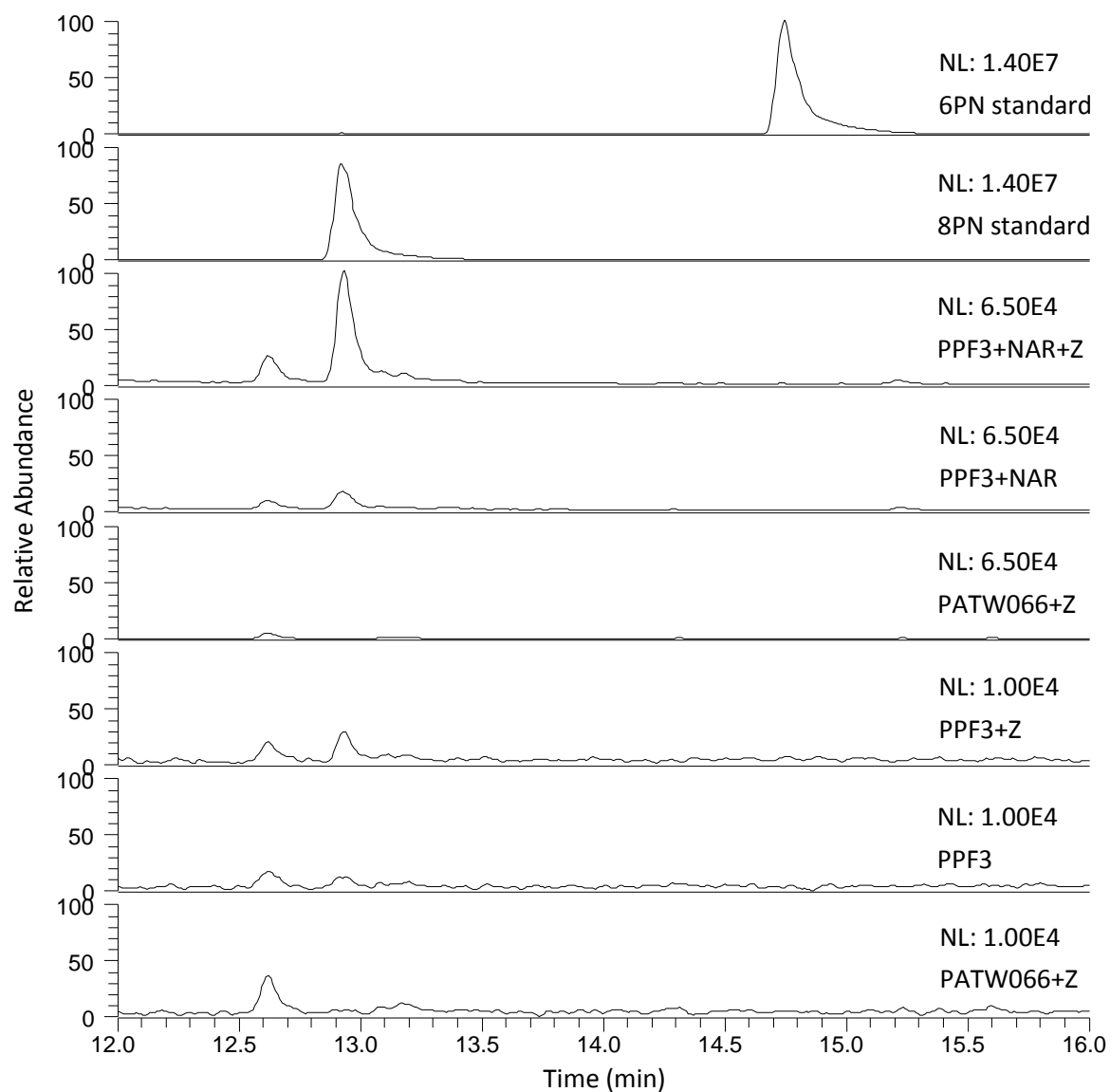
1. Griesbach, R. (2005). Biochemistry and genetics of flower color. *Plant Breeding Reviews*, 25 pp.89-114.
2. Iwashina, T. (2003). Flavonoid Function and Activity to Plants and Other Organisms. *Biological Sciences in Space*, 17(1), pp.24-44.
3. Aoki, T., Akashi, T. and Ayabe, S. (2000). Flavonoids of Leguminous Plants: Structure, Biological Activity, and Biosynthesis. *Journal of Plant Research*, 113(4), pp.475-488.
4. Orhan, D., Özçelik, B., Özgen, S. and Ergun, F. (2010). Antibacterial, antifungal, and antiviral activities of some flavonoids. *Microbiological Research*, 165(6), pp.496-504.
5. Banjarnahor, S. and Artanti, N. (2014). Antioxidant properties of flavonoids. *Medical Journal of Indonesia*, 23(4), pp.239-244.
6. Yamamoto, Y. and Gaynor, R. (2001). Therapeutic potential of inhibition of the NF- κ B pathway in the treatment of inflammation and cancer. *Journal of Clinical Investigation*, 107(2), pp.135-142.
7. Manach, C., Mazur, A. and Scalbert, A. (2005). Polyphenols and prevention of cardiovascular diseases. *Current Opinion in Lipidology*, 16(1), pp.77-84.
8. Tangney, C. and Rasmussen, H. (2013). Polyphenols, Inflammation, and Cardiovascular Disease. *Current Atherosclerosis Reports*, 15(5), pp.324-333.
9. Middleton, E. and Kandaswami, C. (1992). Effects of flavonoids on immune and inflammatory cell functions. *Biochemical Pharmacology*, 43(6), pp.1167-1179.
10. Kumar, S. and Pandey, A. (2013). Chemistry and Biological Activities of Flavonoids: An Overview. *The Scientific World Journal*, 2013, pp.1-16.
11. Ferriola, P., Cody, V. and Middleton, E. (1989). Protein kinase C inhibition by plant flavonoids. *Biochemical Pharmacology*, 38(10), pp.1617-1624.
12. Cazarolli, L., Zanatta, L., Alberton, E., Bonorino Figueiredo, M., Folador, P., Damazio, R., Pizzolatti, M. and Barreto Silva, F. (2008). Flavonoids: Prospective Drug Candidates. *Mini-Reviews in Medicinal Chemistry*, 8(13), pp.1429-1440.
13. Quattrocchio, F., Baudry, A., Lepiniec, L. and Grotewold, E. (2006). The Regulation of Flavonoid Biosynthesis. *The Science of Flavonoids*, pp.97-122.
14. Bohlmann, F. and Gören, N. (1984). Three prenylated flavanoids from *Helichrysum athrixifolium*. *Phytochemistry*, 23(6), pp.1338-1339.
15. Park, K., You, J., Lee, H., Baek, N. and Hwang, J. (2003). Kuwanon G: an antibacterial agent from the root bark of *Morus alba* against oral pathogens. *Journal of Ethnopharmacology*, 84(2-3), pp.181-185.
16. Stevens, J., Taylor, A., Nickerson, G., Ivancic, M., Henning, J., Haunold, A. and Deinzer, M. (2000). Prenylflavonoid variation in *Humulus lupulus*: distribution and taxonomic significance of xanthogalenol and 4'-O-methylxanthohumol. *Phytochemistry*, 53(7), pp.759-775.
17. Son, J., Park, J., Kim, J., Kim, Y., Chung, S. and Lee, S. (2003). Prenylated Flavonoids from the Roots of *Sophora flavescens* with Tyrosinase Inhibitory Activity. *Planta Medica*, 69(6), pp.559-561.
18. Botta, B., Vitali, A., Menendez, P., Misiti, D. and Monache, G. (2005). Prenylated Flavonoids: Pharmacology and Biotechnology. *Current Medicinal Chemistry*, 12(6), pp.713-739.
19. Araya-Cloutier, C., Martens, B., Schaftenaar, G., Leipoldt, F., Gruppen, H. and Vincken, J. (2017). Structural basis for non-genuine phenolic acceptor substrate specificity of *Streptomyces roseochromogenes* prenyltransferase CloQ from the ABBA/PT-barrel superfamily. *PLOS ONE*, 12(3), p.e0174665.
20. Kuzuyama, T., Noel, J. and Richard, S. (2005). Structural basis for the promiscuous biosynthetic prenylation of aromatic natural products. *Nature*, 435(7044), pp.983-987.
21. Ozaki, T., Mishima, S., Nishiyama, M. and Kuzuyama, T. (2009). NovQ is a prenyltransferase capable of catalyzing the addition of a dimethylallyl group to both phenylpropanoids and flavonoids. *The Journal of Antibiotics*, 62(7), pp.385-392.
22. Kumazawa, S., Ueda, R., Hamasaka, T., Fukumoto, S., Fujimoto, T. and Nakayama, T. (2007). Antioxidant Prenylated Flavonoids from Propolis Collected in Okinawa, Japan. *Journal of Agricultural and Food Chemistry*, 55(19), pp.7722-7725.
23. Chen, X., Mukwaya, E., Wong, M. and Zhang, Y. (2013). A systematic review on biological activities of prenylated flavonoids. *Pharmaceutical Biology*, 52(5), pp.655-660.
24. Araya-Cloutier, C., Gruppen, H., Vincken, J. and Besten, H. (2017). *Antibacterial prenylated isoflavonoids and stilbenoids*.

25. Yang, X., Jiang, Y., Yang, J., He, J., Sun, J., Chen, F., Zhang, M. and Yang, B. (2015). Prenylated flavonoids, promising nutraceuticals with impressive biological activities. *Trends in Food Science & Technology*, 44(1), pp.93-104.
26. Mizobuchi, S. and Sato, Y. (1984). A New Flavanone with Antifungal Activity Isolated from Hops. *Agricultural and Biological Chemistry*, 48(11), pp.2771-2775.
27. Verzele, M., Stockx, J., Fontijn, F. and Anteunis, M. (2010). Xanthohumol, a New Natural Chalkone. *Bulletin des Sociétés Chimiques Belges*, 66(1), pp.452-475.
28. Stevens, J. and Page, J. (2004). Xanthohumol and related prenylflavonoids from hops and beer: to your good health!. *Phytochemistry*, 65(10), pp.1317-1330.
29. Gao, X., Deeb, D., Liu, Y., Gautam, S., Dulchavsky, S. and Gautam, S. (2009). Immunomodulatory activity of xanthohumol: inhibition of T cell proliferation, cell-mediated cytotoxicity and Th1 cytokine production through suppression of NF- κ B. *Immunopharmacology and Immunotoxicology*, 31(3), pp.477-484.
30. Gerhauser, C., Alt, A., Heiss, E., Gamal-Eldeen, A., Klimo, K., Knauff, J., Neumann, I., Scherf, H., Frank, N., Bartsch, H. and Becker, H. (2002). Cancer Chemopreventive Activity of Xanthohumol, a Natural Product Derived from Hop. *Molecular Cancer Therapeutics*, 1(11), pp.959-969.
31. Colgate, E., Miranda, C., Stevens, J., Bray, T. and Ho, E. (2007). Xanthohumol, a prenylflavonoid derived from hops induces apoptosis and inhibits NF-kappaB activation in prostate epithelial cells. *Cancer Letters*, 246(1-2), pp.201-209.
32. Milligan, S. (2000). The Endocrine Activities of 8-Prenylnaringenin and Related Hop (*Humulus lupulus* L.) Flavonoids. *Journal of Clinical Endocrinology & Metabolism*, 85(12), pp.4912-4915.
33. Brunelli, E., Minassi, A., Appendino, G. and Moro, L. (2007). 8-Prenylnaringenin, inhibits estrogen receptor- α mediated cell growth and induces apoptosis in MCF-7 breast cancer cells. *The Journal of Steroid Biochemistry and Molecular Biology*, 107(3-5), pp.140-148.
34. Matsumura, A., Ghosh, A., Pope, G. and Darbre, P. (2005). Comparative study of oestrogenic properties of eight phytoestrogens in MCF7 human breast cancer cells. *The Journal of Steroid Biochemistry and Molecular Biology*, 94(5), pp.431-443.
35. Wang, Y., Chen, S. and Yu, O. (2011). Metabolic engineering of flavonoids in plants and microorganisms. *Applied Microbiology and Biotechnology*, 91(4), pp.949-956.
36. Leonard, E., Lim, K., Saw, P. and Koffas, M. (2007). Engineering Central Metabolic Pathways for High-Level Flavonoid Production in *Escherichia coli*. *Applied and Environmental Microbiology*, 73(12), pp.3877-3886.
37. Trantas, E., Panopoulos, N. and Ververidis, F. (2009). Metabolic engineering of the complete pathway leading to heterologous biosynthesis of various flavonoids and stilbenoids in *Saccharomyces cerevisiae*. *Metabolic Engineering*, 11(6), pp.355-366.
38. Santos, C., Koffas, M. and Stephanopoulos, G. (2011). Optimization of a heterologous pathway for the production of flavonoids from glucose. *Metabolic Engineering*, 13(4), pp.392-400.
39. Koopman, F., Beekwilder, J., Crimi, B., van Houwelingen, A., Hall, R., Bosch, D., van Maris, A., Pronk, J. and Daran, J. (2012). De novo production of the flavonoid naringenin in engineered *Saccharomyces cerevisiae*. *Microbial Cell Factories*, 11(1), p.155-169.
40. Jiang, H. and Morgan, J. (2003). Optimization of an in vivo plant P450 monooxygenase system in *Saccharomyces cerevisiae*. *Biotechnology and Bioengineering*, 85(2), pp.130-137.
41. Ralston, L. (2005). Partial Reconstruction of Flavonoid and Isoflavonoid Biosynthesis in Yeast Using Soybean Type I and Type II Chalcone Isomerases. *Plant Physiology*, 137(4), pp.1375-1388.
42. Sasaki, K., Tsurumaru, Y. and Yazaki, K. (2009). Prenylation of Flavonoids by Biotransformation of Yeast Expressing Plant Membrane-Bound Prenyltransferase SfN8DT-1. *Bioscience, Biotechnology, and Biochemistry*, 73(3), pp.759-761.
43. Chen, R., Liu, X., Zou, J., Yin, Y., Ou, B., Li, J., Wang, R., Xie, D., Zhang, P. and Dai, J. (2013). Regio- and Stereospecific Prenylation of Flavonoids by *Sophora flavescens* Prenyltransferase. *Advanced Synthesis & Catalysis*, 355(9), pp.1817-1828.
44. Tsurumaru, Y., Sasaki, K., Miyawaki, T., Uto, Y., Momma, T., Umemoto, N., Momose, M. and Yazaki, K. (2012). HIPT-1, a membrane-bound prenyltransferase responsible for the biosynthesis of bitter acids in hops. *Biochemical and Biophysical Research Communications*, 417(1), pp.393-398.
45. Nagel, J., Culley, L., Lu, Y., Liu, E., Matthews, P., Stevens, J. and Page, J. (2008). EST Analysis of Hop Glandular Trichomes Identifies an O-Methyltransferase That Catalyzes the Biosynthesis of Xanthohumol. *The Plant Cell Online*, 20(1), pp.186-200.

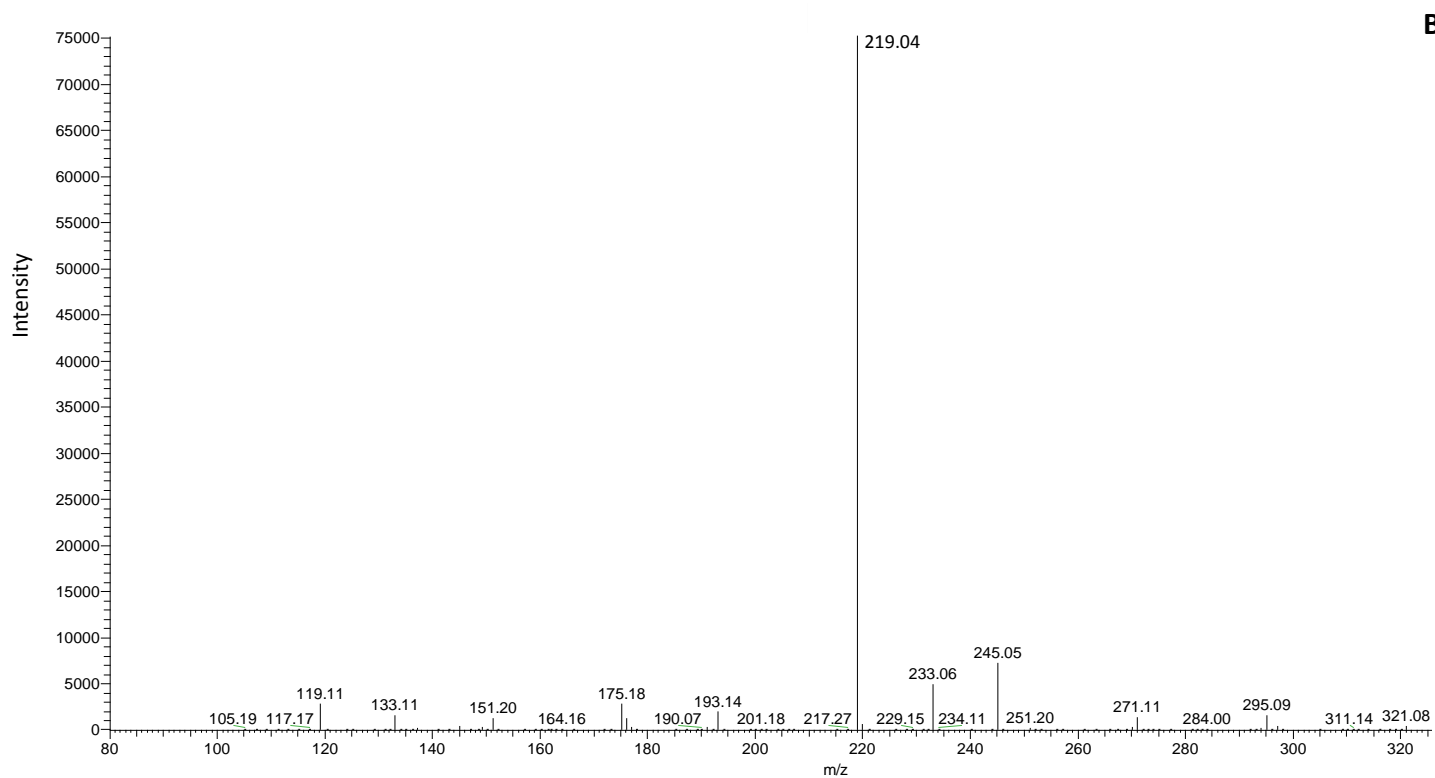
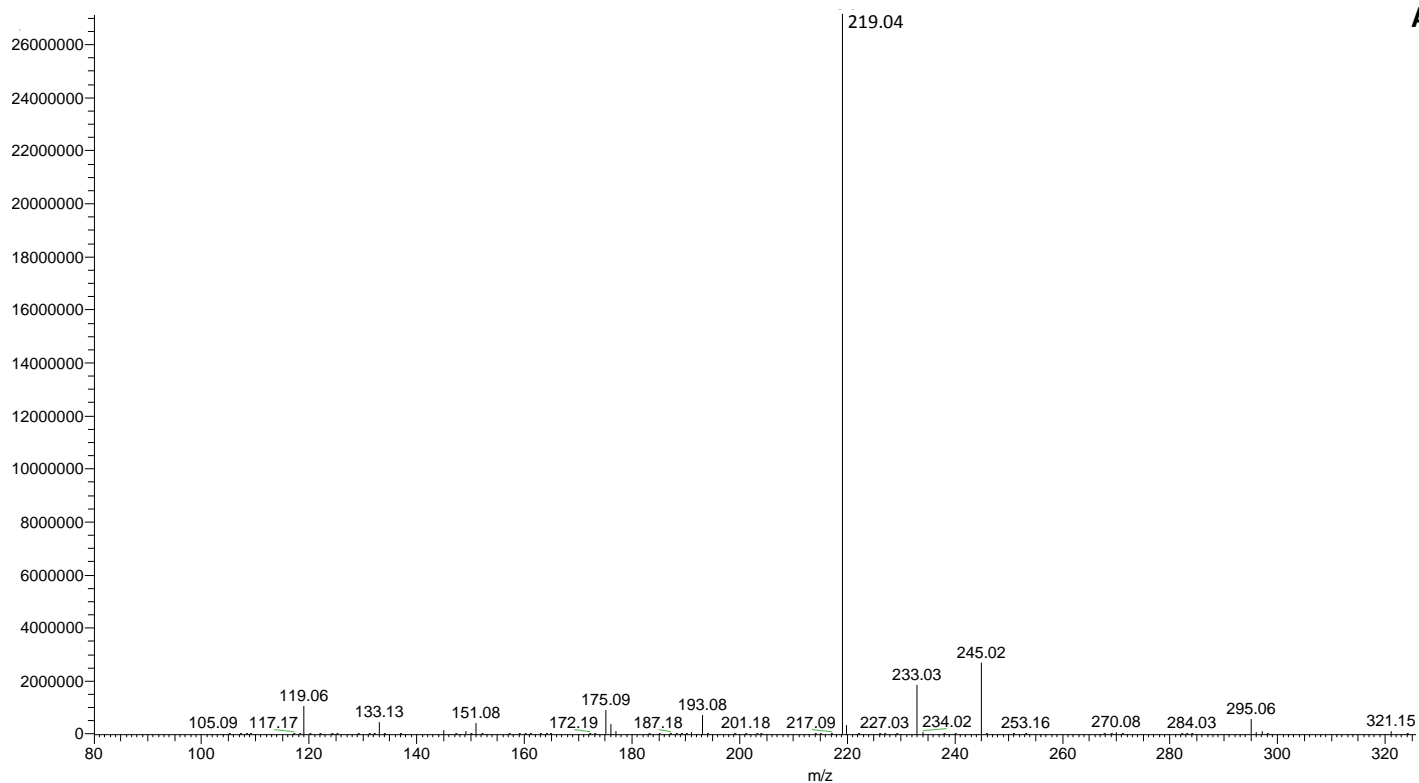
46. Shen, G., Huhman, D., Lei, Z., Snyder, J., Sumner, L. and Dixon, R. (2012). Characterization of an Isoflavonoid-Specific Prenyltransferase from *Lupinus albus*. *Plant Physiology*, 159(1), pp.70-80.
47. Akashi, T., Sasaki, K., Aoki, T., Ayabe, S. and Yazaki, K. (2008). Molecular Cloning and Characterization of a cDNA for Pterocarpan 4-Dimethylallyltransferase Catalyzing the Key Prenylation Step in the Biosynthesis of Glyceollin, a Soybean Phytoalexin. *Plant Physiology*, 149(2), pp.683-693.
48. Brown, S., Clastre, M., Courdavault, V. and O'Connor, S. (2015). De novo production of the plant-derived alkaloid strictosidine in yeast. *Proceedings of the National Academy of Sciences*, 112(11), pp.3205-3210.
49. Levisson, M., Patinios, C., Hein, S., de Groot, P., Daran, J., Hall, R., Martens, S. and Beekwilder, J. (2018). Engineering de novo anthocyanin production in *Saccharomyces cerevisiae*. *Microbial Cell Factories*, 17(1), pp.103-118.
50. Eichenberger, M., Lehka, B., Folly, C., Fischer, D., Martens, S., Simón, E. and Naesby, M. (2017). Metabolic engineering of *Saccharomyces cerevisiae* for de novo production of dihydrochalcones with known antioxidant, antidiabetic, and sweet tasting properties. *Metabolic Engineering*, 39, pp.80-89.
51. Lehka, B., Eichenberger, M., Bjørn-Yoshimoto, W., Vanegas, K., Buijs, N., Jensen, N., Dyekjær, J., Jenssen, H., Simon, E. and Naesby, M. (2017). Improving heterologous production of phenylpropanoids in *Saccharomyces cerevisiae* by tackling an unwanted side reaction of Tsc13, an endogenous double bond reductase. *FEMS Yeast Research*, 17(1).
52. Wang, H., Yang, Y., Lin, L., Zhou, W., Liu, M., Cheng, K. and Wang, W. (2016). Engineering *Saccharomyces cerevisiae* with the deletion of endogenous glucosidases for the production of flavonoid glucosides. *Microbial Cell Factories*, 15(1), pp.134-145.
53. N.M. Mol, J., P. Robbinst, M., A. Dixon, R. and Veltkamp, E. (1985). Spontaneous and enzymic rearrangement of naringenin chalcone to flavanone. *Phytochemistry*, 24(10), pp.2267-2269.
54. Wunderlich, S., Zürcher, A. and Back, W. (2005). Enrichment of xanthohumol in the brewing process. *Molecular Nutrition & Food Research*, 49(9), pp.874-881.
55. Stevens, J., Taylor, A., Clawson, J. and Deinzer, M. (1999). Fate of Xanthohumol and Related Prenylflavonoids from Hops to Beer. *Journal of Agricultural and Food Chemistry*, 47(6), pp.2421-2428.
56. Chen, W., Becker, T., Qian, F. and Ring, J. (2013). Beer and beer compounds: physiological effects on skin health. *Journal of the European Academy of Dermatology and Venereology*, 28(2), pp.142-150.
57. Li, H., Ban, Z., Qin, H., Ma, L., King, A. and Wang, G. (2015). A Heteromeric Membrane-Bound Prenyltransferase Complex from Hop Catalyzes Three Sequential Aromatic Prenylations in the Bitter Acid Pathway. *Plant Physiology*, 167(3), pp.650-659.
58. Shen, G., Huhman, D., Lei, Z., Snyder, J., Sumner, L. and Dixon, R. (2012). Characterization of an Isoflavonoid-Specific Prenyltransferase from *Lupinus albus*. *Plant Physiology*, 159(1), pp.70-80.
59. Sasaki, K., Tsurumaru, Y., Yamamoto, H. and Yazaki, K. (2011). Molecular Characterization of a Membrane-bound Prenyltransferase Specific for Isoflavone from *Sophora flavescens*. *Journal of Biological Chemistry*, 286(27), pp.24125-24134.
60. Sasaki, K., Mito, K., Ohara, K., Yamamoto, H. and Yazaki, K. (2008). Cloning and Characterization of Naringenin 8-Prenyltransferase, a Flavonoid-Specific Prenyltransferase of *Sophora flavescens*. *Plant Physiology*, 146(3), pp.1075-1084.
61. Ban, Z., Qin, H., Mitchell, A., Liu, B., Zhang, F., Weng, J., Dixon, R. and Wang, G. (2018). Noncatalytic chalcone isomerase-fold proteins in *Humulus lupulus* are auxiliary components in prenylated flavonoid biosynthesis. *Proceedings of the National Academy of Sciences*, 115(22), pp.E5223-E5232.
62. Entian, K. and Kötter, P. (2007). 25 Yeast Genetic Strain and Plasmid Collections. *Methods in Microbiology*, 36, pp.629-666.
63. Lööke, M., Kristjuhan, K. and Kristjuhan, A. (2011). Extraction of genomic DNA from yeasts for PCR-based applications. *BioTechniques*, 50(5), pp.325-328.
64. Kuijpers, N., Solis-Escalante, D., Bosman, L., van den Broek, M., Pronk, J., Daran, J. and Daran-Lapujade, P. (2013). A versatile, efficient strategy for assembly of multi-fragment expression vectors in *Saccharomyces cerevisiae* using 60 bp synthetic recombination sequences. *Microbial Cell Factories*, 12(1), p.47.
65. Grote, A., Hiller, K., Scheer, M., Munch, R., Nortemann, B., Hempel, D. and Jahn, D. (2005). JCat: a novel tool to adapt codon usage of a target gene to its potential expression host. *Nucleic Acids Research*, 33(Web Server), pp.W526-W531.
66. Daniel Gietz, R. and Woods, R. (2002). Transformation of yeast by lithium acetate/single-stranded carrier DNA/polyethylene glycol method. *Guide to Yeast Genetics and Molecular and Cell Biology - Part B*, 350, pp.87-96.

67. DiCarlo, J., Norville, J., Mali, P., Rios, X., Aach, J. and Church, G. (2013). Genome engineering in *Saccharomyces cerevisiae* using CRISPR-Cas systems. *Nucleic Acids Research*, 41(7), pp.4336-4343.
68. Mans, R., van Rossum, H., Wijsman, M., Backx, A., Kuijpers, N., van den Broek, M., Daran-Lapujade, P., Pronk, J., van Maris, A. and Daran, J. (2015). CRISPR/Cas9: a molecular Swiss army knife for simultaneous introduction of multiple genetic modifications in *Saccharomyces cerevisiae*. *FEMS Yeast Research*, 15(2).
69. ATUM. (2018). *CRISPR gRNA Design tool - ATUM*. [online] Available at: <https://www.atum.bio/eCommerce/cas9/input>.

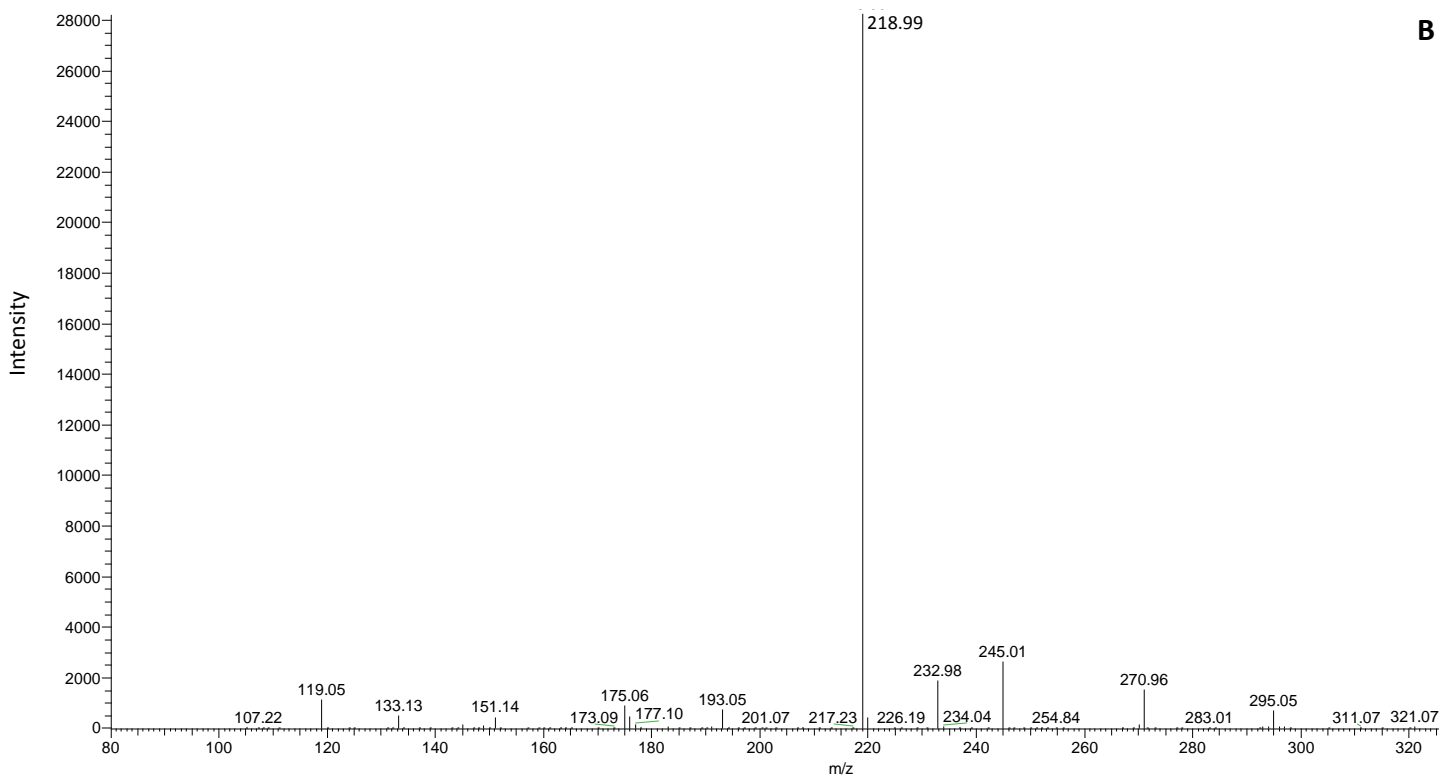
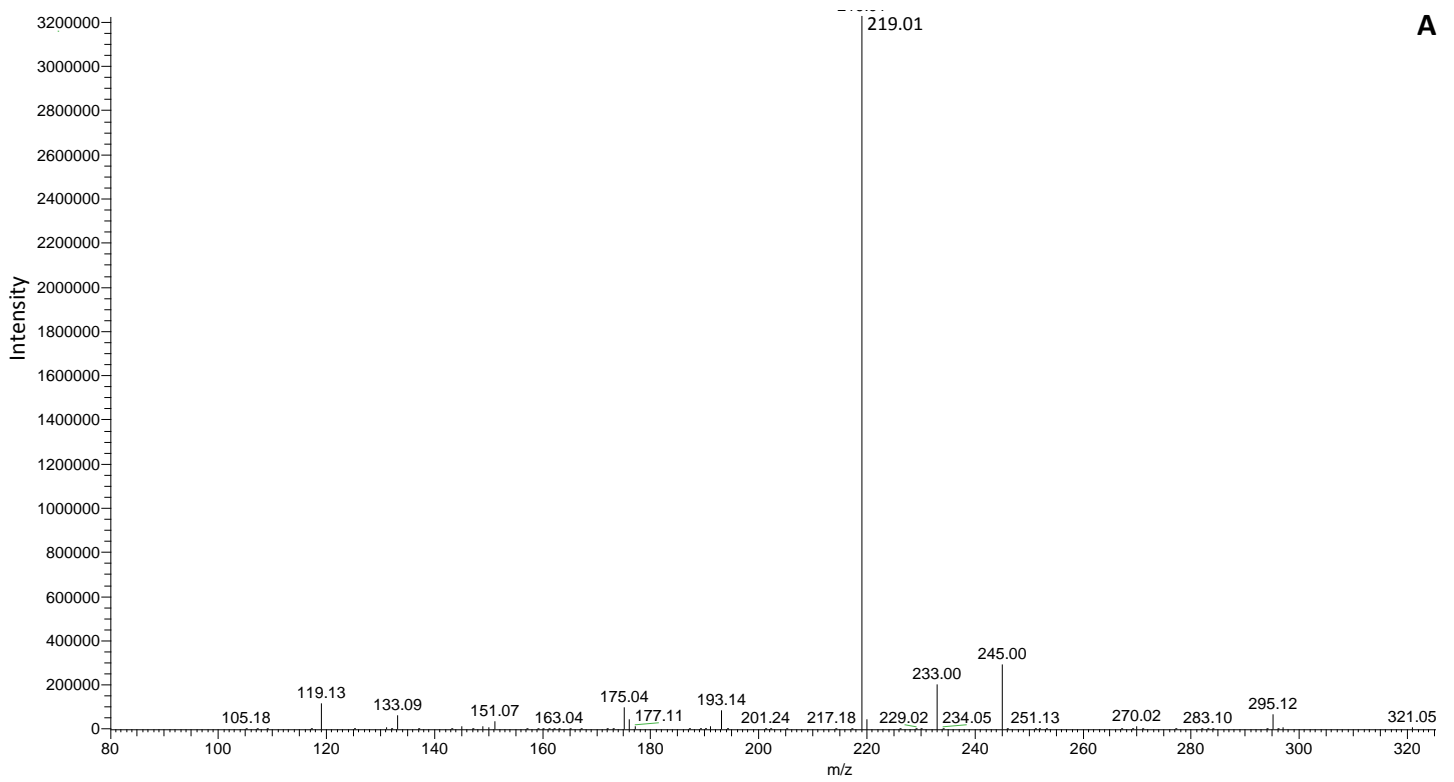
Supplementary Files



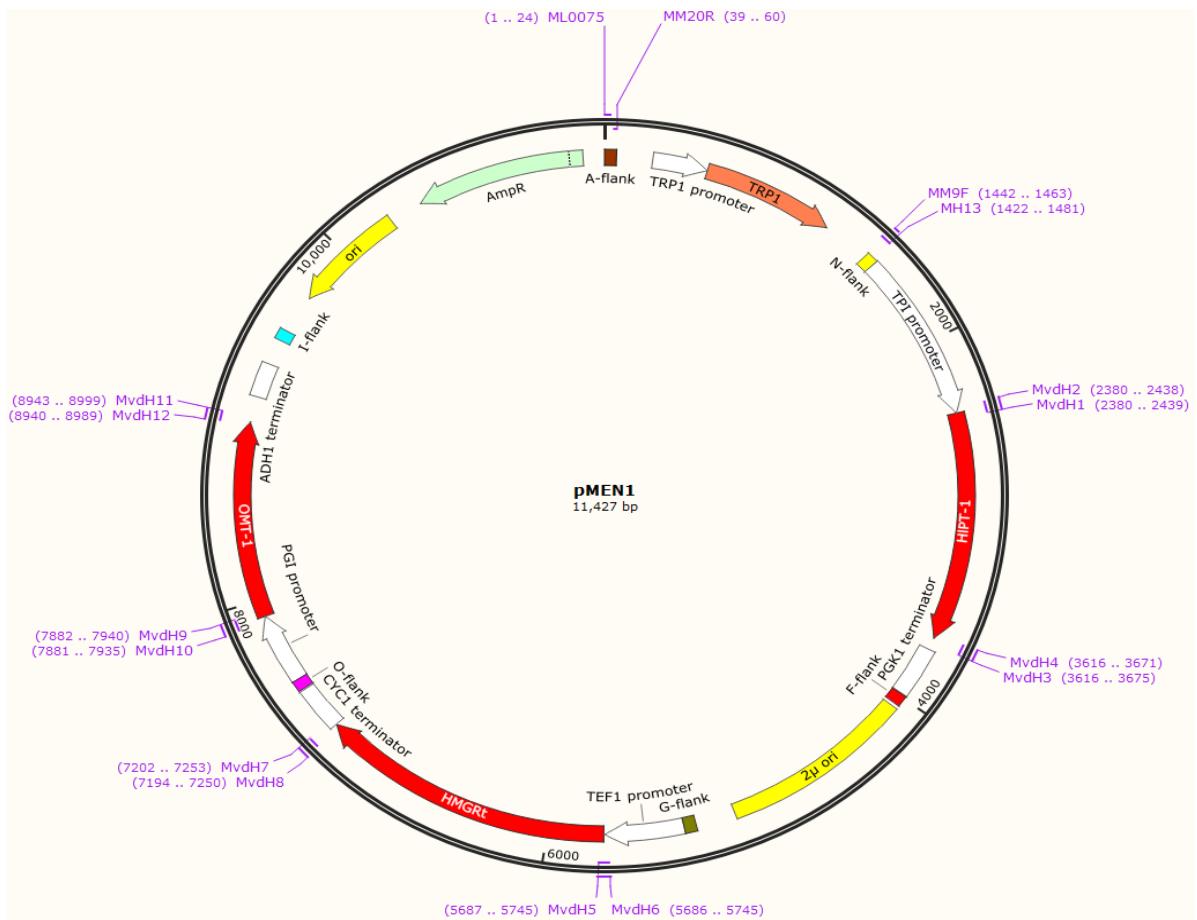
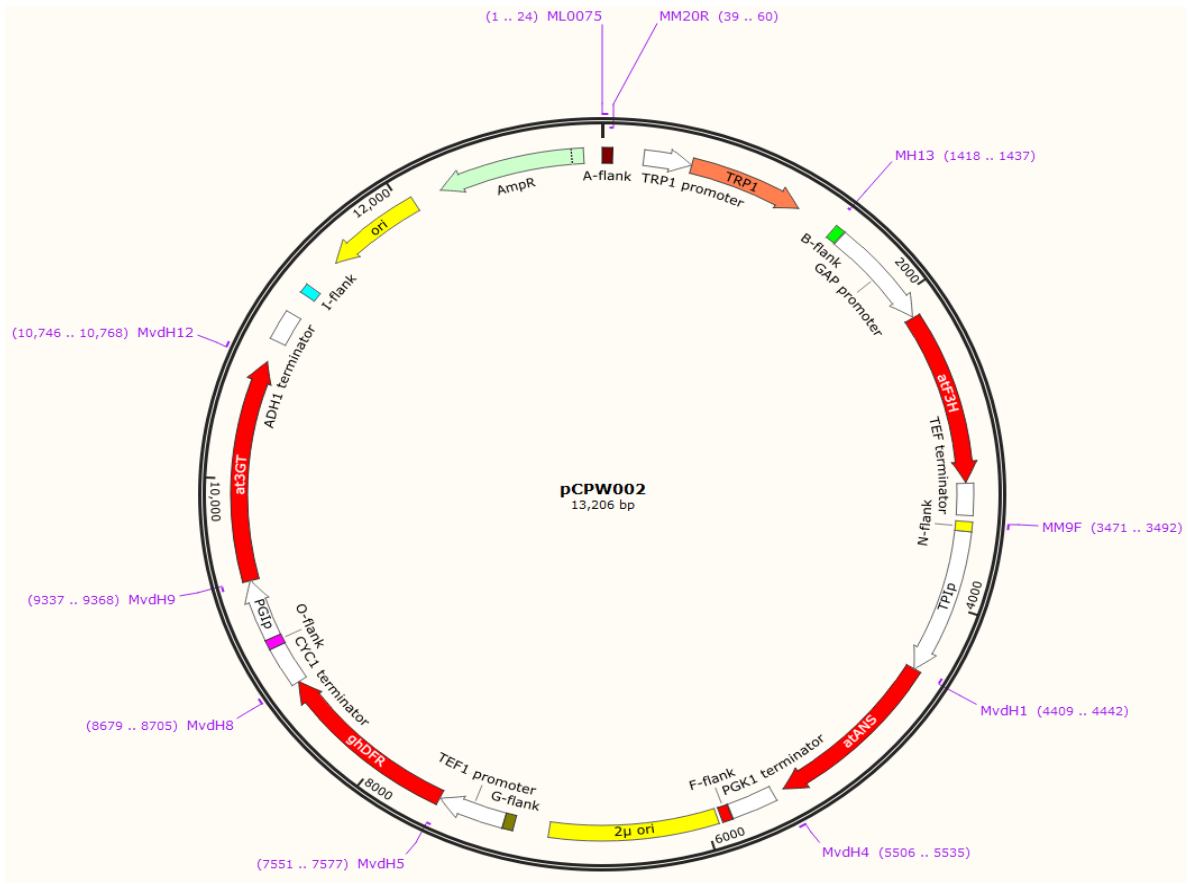
Supplementary Figure 1. LC-MS analysis of 8-prenylnaringenin in the cell pellet of strains PPF3 and PATW066. All strains were cultured in 50 ml SMG medium for 120 hours. Strain PPF3 was additionally cultured with supplementation of naringenin. The supernatant was separated from the cell pellet by centrifugation. Half of the cell pellet samples were treated with Zymolyase and then used for extraction with ethyl acetate and finally analyzed by LC-MS in negative mode. Detection of 8-prenylnaringenin at RT: 12.92 min and m/z : 339. 8-prenylnaringenin and 6-prenylnaringenin standards were used at 0.25 M. NAR, naringenin; Z, Zymolyase.



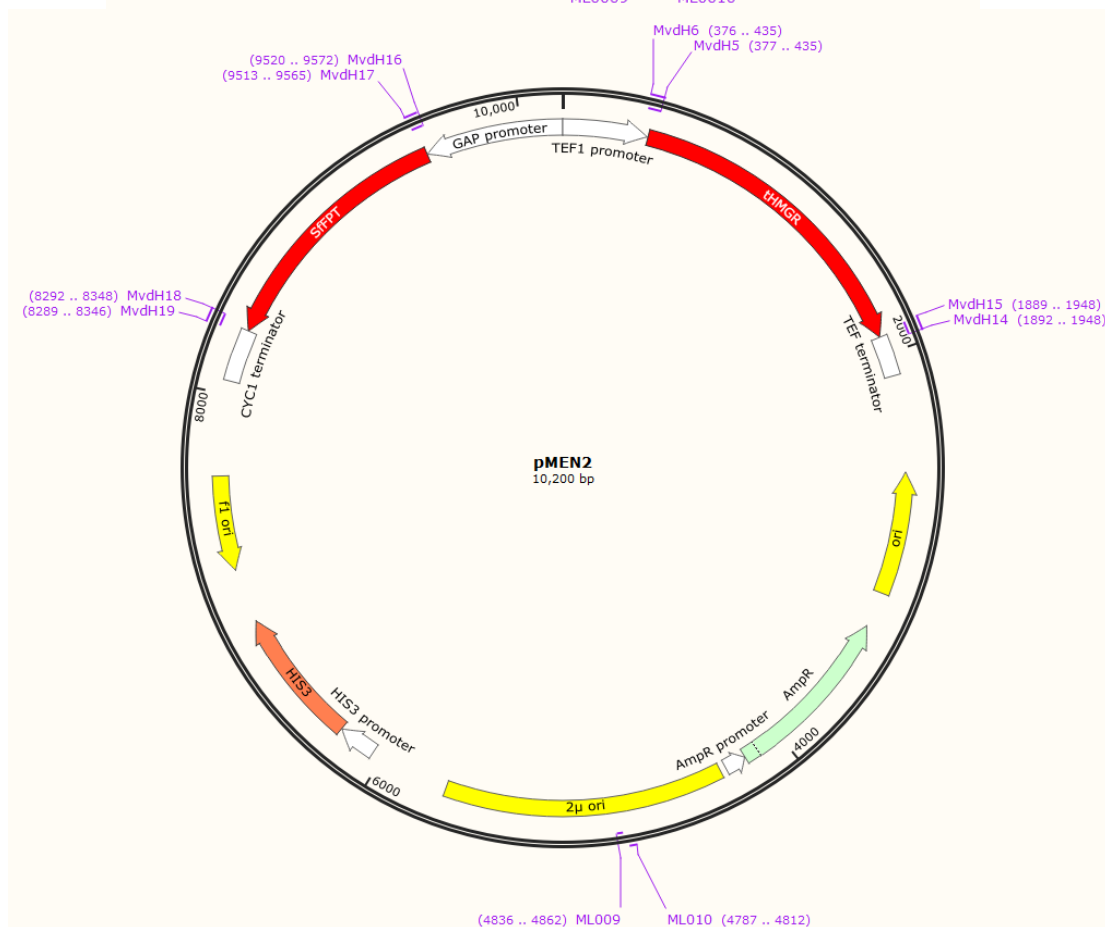
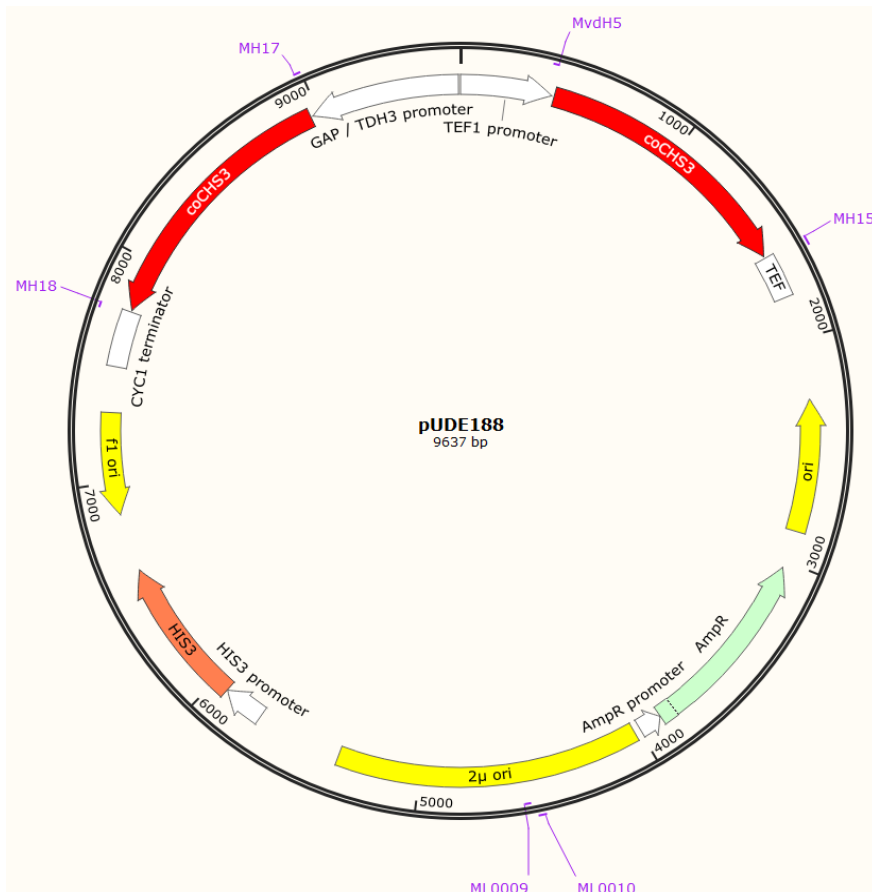
Supplementary Figure 2. MS² spectra of the 8-prenylnaringenin (m/z 339) standard (**A**) and 8-prenylnaringenin found in the PPF3+NAR supernatant sample (**B**).



Supplementary Figure 3. MS² spectra of the 8-prenylnaringenin (*m/z* 339) standard (**A**) and 8-prenylnaringenin found in the PPF3+NAR+Z pellet sample (**B**).



Supplementary Figure 4. Plasmids pCPW002 and pMEN1. pCPW002 was used as backbone for pMEN1



Supplementary Figure 5. Plasmids pUDE188 and pMEN2. pUDE188 was used as backbone for pMEN2

Supplementary Table 1

Oligonucleotide primers used in this study

Primer name	Sequence (5'-3')	Description
Plasmid construction primers		
MvdH1	AGAGAAAGAAGAAACAGAAGACAATTCCATATGTGTTTTTTGTAGTTATAGATTTAAGCA	N-TPIp-rv
MvdH2	TGCTTAAATCTATAACTACAAAAACACATATGGAATTGTCTTCTGTTTCTTCTTTCTC	HIPT-fw
MvdH3	AATTCCTTACCTTCCAATAATTCCAAAGAATTAGATGAACAAGTAAACAACGTATTGAGC	HIPT-rv
MvdH4	GCTGAATACGTTGTTTACTTGTTTCATCTAATTCTTTGGAATTATTGGAAGGTAAGG	PGK1t-2 μ -TEF1p-fw
MvdH5	CAGAAATGACTGTTTTATTGGTTAAAACATAAAACTTAGATTAGATTGCTATGCTTTC	PGK1t-2 μ -TEF1p-rv / GAPp-TEF1p-rv
MvdH6	AGAAAGCATAGCAATCTAATCTAAGTTTTATGGTTTTAACCAATAAAACAGTCATTTCTG	HMGrt-fw / HMGrt2-fw
MvdH7	AATGTAAGCGTGACATAACTAATTACATGATTAGGATTTAATGCAGGTGACG	HMGrt-rv
MvdH8	GATGGGTCCGTCACCTGCATTAATCCTAATCATGTAATTAGTTATGTCACGCTTAC	CYC1t-O-PGIp-fw
MvdH9	GATTTGTTCTTGACCTCTCAAAGATTCCATTTTTAGGCTGGTATCTTGATTCTAAATCG	CYC1t-O-PGIp-rv
MvdH10	TCGATTTAGAATCAAGATACCAGCCTAAAAATGGAATCTTTGAGAGGTCAAGAAC	OMT1-fw
MvdH11	CAAACCTCTGGCGAAGAAGTCCAAAGCTTCTAAACCAAGAAAGCTTCGATGATAGC	OMT1-rv
MvdH12	CCAGCTATCATCGAAGCTTTCTTGGTTAAGAAGCTTTGGACTTCTTCGC	ADH1t-AmpR-A-fw
MH13	TCCACATATCTTCGTTAGGACTCAATCGTGGCTGCTGATCCTGGAACAACACTCAACCCT	A-TRP1-N-rv
MH14	GACAAGTTCTTGAAAACAAGAATCTTTTTATTGTCTTAGGATTTAATGCAGGTGACG	HMGrt2-rv
MH15	GTCCGTCACCTGCATTAATCCTAAGACAATAAAAAGATTCTTGTTTTCAAGAACTTGTC	TEF1t-AmpR-2 μ -fw
MH16	AAAACACCAGAACTTAGTTTCGACGGATTTCATGGGTTCTATGTTGTTGGCTTC	SfFPT-rv
MH17	TGGGAAAGAAGCCAACAACATAGAACCCATGAATCCGTCGAAACTAAGTTCTG	GAPp-TEF1p-fw
MH18	GACTACTTCTTGATCCCATTGTTTCAGATAATCATGTAATTAGTTATGTCACGCTTAC	2 μ -HIS3-CYC1t-fw
MH19	AATGTAAGCGTGACATAACTAATTACATGATTATCTGAACAATGGGATCAAGAAGT	SfFPT-fw
ML0009	TCGGTATAGAATATAATCGGGGATGCC	TEF1t-AmpR-2 μ -rv / 2 μ -AmpR-SNR52p- GTS-fw
ML0010	GCGTTTACTGATTACTAGCGAAGCTG	2 μ -HIS3-CYC1t-fw / 2 μ -URA3-SUP4t- GTS-rv
ML0075	ACTATATGTGAAGGCATGGCTATG	A-TRP1-N-fw
MM9F	GATCAGCAGCCACGATTGAGTC	N-TPIp-fw

MM20R	GTGCCTATTGATGATCTGGCGG	ADH1t-AmpR-A-rv
Genomic integration primers		
CP169	CTTCAAAGCAAATTTTCAATCTTCCATGTCAATAACTGGACCTAACGGTTCATTGAG GCAAATTAAGCCTTCGAGC	SPR1-GAPp-coTAL- CYC1t-rv
CP171	GCAAATTAAGCCTTCGAGC	GAPp-coTAL-CYC1t- rv
CP190	ACACCTTCTTTATTCGAGACTTCCGTAATAATCCGTACAACGATGACGGTATTCTGTT TGTAACGACGGCCAGT	SPR1-GAPp-coTAL- CYC1t-fw
MH24	TGTAGGTCAGGTTGCTTCTC	ADH1t-fw / ADH1t-X-2bdown- fw
MH25	CAAAGCCGATAAGAAAAAGATGGAAGAACGATTACAACAGGTG	ADH1t-rv
MH26	CTGTTGTAATCGTCTTCCATCTTTTCTTATCGGCTTGTGC	X-2bdown-fw
MH27	GTCGGTTGTACGCCATTAC	X-2bdown-rv / ADH1t-X-2bdown-rv
ML0017	TGTAACGACGGCCAGT	GAPp-coTAL-CYC1t- fw
gRNA replacement primers		
MH22	GATCGGGAAGAACGGTGTGCACCGTTTTAGAGCTAGAAATAGC	CHI-GTS-fw
MH23	CTAAACGGTGACACACCGTTCTCCCGATCATTTATCTTTCAGTGC	CHI-GTS-rv
Verification primers		
CP23	AAAGGGAATAAGGGCGACAC	A-TRP1-N-diagnosis- fw
CP28	CCTGAATAAAGTCTCTTGAAACTGG	A-TRP1-N-diagnosis- rv
CP30	TGAAGCACAGATTCTTCGTTGG	<i>HIPT1</i> -diagnosis-rv
CP100	CGGTCTCAATTTCTCAAGTTTCAG	<i>HMGRt</i> -diagnosis-fw
CP102	CTCCTCCTTTTCGGTTAGAGC	<i>SfFPT</i> -diagnosis-fw
CP162	GGTGGTGGCTAGTATTGGAG	<i>coTAL1</i> -diagnosis-fw
CP163	GATGGTCAATTATGACGCCATATTCG	<i>coTAL1</i> -diagnosis-rv
CP184	TGAAAAGGGACTAAGAGCGTG	<i>coMdECR</i> -diagnosis- fw
CP185	GATGAAAGCACCGAAAGACC	<i>coMdECR</i> - internaldiagnosis-rv
CP186	GACTTTGCCAGTTCAACCAGG	<i>coMdECR</i> - internaldiagnosis-fw
CP187	TGCTACTACGCCACTTCGTG	<i>coMdECR</i> -diagnosis- rv
MH20	GGGTCTCTAACTTGTGGTTCG	<i>SfFPT/HMGRt</i> - internaldiagnosis-fw

MH21	GATGCTAATACAGGAGCTTCTGC	<i>SfFPT/HMGRt</i> - internaldiagnosis-rv
MM25F	CTCTTAGCGCAACTACAGAGAACAGG	<i>SfFPT</i> -diagnosis-rv
MM28R	ACCAGCATTACATACGATTGACG	<i>HMGRt</i> -diagnosis-rv
MM29F	ACGGGAGCGTAATGGTGATG	<i>HIPT1</i> -diagnosis-fw
MM38R	TGGTCAATAAGAGCGACCTCATG	<i>OMT1</i> -diagnosis-rv
MM91F	CAGACGGAATTTCCCTATTTGTTTCG	<i>OMT1</i> -diagnosis-fw